

Systems Genetics Implicates Cytoskeletal Genes in Oocyte Control of Cloned Embryo Quality

Yong Cheng,* John Gaughan,[†] Uros Midic,* Zhiming Han,* Cheng-Guang Liang,* Bela G. Patel,*
and Keith E. Latham*^{*,†,1}

*The Fels Institute for Cancer Research and Molecular Biology, Philadelphia, Pennsylvania 19140, and [†]The Biostatistics Consulting Center and [†]The Department of Biochemistry, Temple University School of Medicine, Philadelphia, Pennsylvania 19140

ABSTRACT Cloning by somatic cell nuclear transfer is an important technology, but remains limited due to poor rates of success. Identifying genes supporting clone development would enhance our understanding of basic embryology, improve applications of the technology, support greater understanding of establishing pluripotent stem cells, and provide new insight into clinically important determinants of oocyte quality. For the first time, a systems genetics approach was taken to discover genes contributing to the ability of an oocyte to support early cloned embryo development. This identified a primary locus on mouse chromosome 17 and potential loci on chromosomes 1 and 4. A combination of oocyte transcriptome profiling data, expression correlation analysis, and functional and network analyses yielded a short list of likely candidate genes in two categories. The major category—including two genes with the strongest genetic associations with the traits (*Epb4.1B* and *Dlgap1*)—encodes proteins associated with the subcortical cytoskeleton and other cytoskeletal elements such as the spindle. The second category encodes chromatin and transcription regulators (*Runx1t1*, *Smchd1*, and *Chd7*). *Smchd1* promotes X chromosome inactivation, whereas *Chd7* regulates expression of pluripotency genes. *Runx1t1* has not been associated with these processes, but acts as a transcriptional repressor. The finding that cytoskeleton-associated proteins may be key determinants of early clone development highlights potential roles for cytoplasmic components of the oocyte in supporting nuclear reprogramming. The transcriptional regulators identified may contribute to the overall process as downstream effectors.

THE oocyte is a remarkable cell. It harbors essential stored mRNAs, proteins, and other macromolecules to sustain and direct normal development until embryonic gene expression commences and until external nutrient supplies become available. The oocyte also has the unique ability to reprogram somatic cell nuclei to a totipotent state, a capacity that reflects its unique role during normal embryogenesis of uniting the two gamete genomes and converting them into an embryonic genome. A variety of approaches since the late 1800s investigated the nuclear reprogramming capacity of oocytes by manipulating the ooplasm–nucleus dialog, using blastomere ligature experiments, embryo splitting, embryonic cell nuclear transfer, and ultimately somatic cell nuclear transfer (SCNT). These methodologies have also been useful

in determining the timing and mechanisms underlying other processes such as cell-fate restriction and lineage determination in the early embryo. Cloning studies can thus provide unique insight into the early formative processes that are essential to creating each new individual.

Ooplasmic components must mediate a myriad of key events to make cloned embryogenesis possible, and observing the execution of these events in cloned embryos can reveal previously unappreciated aspects of normal development. The first step of the cloning process entails chemical disruption of the cytoskeleton to enable removal of the spindle-chromosome complex (SCC). Next, the SCC is removed and discarded along with associated proteins and other macromolecules. The cytoskeletal architecture, which is key to supporting correct protein trafficking, intracellular signaling, and other essential processes, must eventually be repaired. The SCC-associated factors either are replenished or remain deficient (Miyara *et al.* 2006). Upon introduction of the donor cell nucleus by either fusion or microinjection, the oolemma must be repaired. The oocyte must then disassemble the nuclear envelope of the

Copyright © 2013 by the Genetics Society of America
doi: 10.1534/genetics.112.148866

Manuscript received October 19, 2012; accepted for publication December 31, 2012
Supporting information is available online at <http://www.genetics.org/lookup/suppl/doi:10.1534/genetics.112.148866/-/DC1>.

¹Corresponding author: 3307 North Broad St., Philadelphia, PA 19140. E-mail: klatham@temple.edu

donor nucleus, condense the chromosomes, and form a new pseudo-meiotic SCC (pmSCC) by reestablishing a spindle architecture and gathering the chromosomes onto the metaphase plate. This process recapitulates many key aspects of oocyte maturation, but chromosome homologs are not paired, chromosome congression is slow or incomplete, and the pmSCC is defective in many respects (Miyara *et al.* 2006; Han *et al.* 2010b). Clone development is initiated by the artificial activation of the oocyte, either using electrical pulses or chemical mediators, and the mode of activation can alter later gene expression relative to embryos activated by fertilization (Ozil *et al.* 2006). Polar body extrusion is prevented during the activation process through a second round of cytoskeletal disruption to maintain a diploid chromosome complement. After activation, the cloned embryo must undergo DNA replication and correct mitotic divisions during cleavage stages. Gene transcription must initiate before supportive ooplasmic macromolecules become depleted. The donor genome must be reprogrammed, a process that is believed to initiate with chromosome condensation in the oocyte, but likely continues well into cleavage, given the observed persistent differences between cloned and normal embryonic gene expression (Latham 2005; Vassena *et al.* 2007a,b). Essential epigenetic information must be retained during the reprogramming process, but some epigenetic information may be lost during somatic development and will be absent in cloned embryos. The leisurely pace of nuclear reprogramming relative to the onset of embryonic gene transcription in clones results in many somatic cell-like features being manifested throughout cleavage development (Chung *et al.* 2002; Gao *et al.* 2003). Because normal embryos differ markedly from somatic cells with respect to physiology and *in vitro* culture requirements, the persistence of these somatic characteristics means that cloned embryos likely must adapt to a less than optimum environment *in vitro*, and even *in vivo* following embryo transfer (Gao and Latham 2004; Latham 2004, 2005; Latham *et al.* 2007).

Cloning methodologies have substantial practical value, enabling the propagation of valuable livestock and endangered species, and potentially the production of stem cells for therapeutic application. Since the birth of Dolly in 1996 (Campbell *et al.* 1996), much effort has been invested in attempting to enhance the production of cloned animals by SCNT. Given the complex series of events that must occur for cloning to succeed, it is not surprising that many barriers to cloning success have been identified, including incomplete nuclear reprogramming, failure to reactivate X chromosomes and aberrant X chromosome inactivation, deficiencies in spindle formation and function, aneuploidy, loss of genomic imprints, aberrant regulation of DNA methyltransferases, and somatic cell-like features leading to altered culture requirements and metabolism (Eggan *et al.* 2000; Ohgane *et al.* 2001; Chung *et al.* 2002, 2003; Humpherys *et al.* 2002; Gao *et al.* 2003, 2004; Mann *et al.* 2003; Gao and Latham 2004; Latham 2005; Nolen *et al.* 2005; Miyara *et al.* 2006; Vassena *et al.* 2007a,b; Jiang *et al.* 2008; Han *et al.* 2010b, 2008; Inoue *et al.* 2010; Matoba *et al.* 2011;

Mizutani *et al.* 2012). Deficiencies in spindle formation and embryonic aneuploidy have been addressed at least partially by augmenting the ooplasm supply of spindle-associated proteins (Han *et al.* 2010b). Some genes are imprinted in early embryos but lose their imprints in somatic cells (Ogura *et al.* 2002; Wagschal and Feil 2006; Guillomot *et al.* 2010; Chavatte-Palmer *et al.* 2012). Some imprints are normally retained only in the placenta. The loss of placenta-specific genomic imprinting in somatic donor nuclei could thus affect the placenta in clones. Loss of other imprints cell type specifically could affect cloning outcome in a donor cell type-specific manner. No clear remedy to imprinting defects or other defects has emerged. Limitations in nuclear reprogramming have remained a significant barrier in cloning by SCNT and have consequently received a great deal of attention by those seeking to enhance outcomes. Chemical agents that modify chromatin structure and alterations in the methods for removing the recipient oocyte spindle and chromatin have enhanced success in some situations (Akagi *et al.* 2011; Bui *et al.* 2011; Jafari *et al.* 2011; Kim *et al.* 2011; Wang *et al.* 2011; Whitworth *et al.* 2011; Terashita *et al.* 2012). However, while exogenous chemicals or genetic manipulations of donor cell gene expression may enhance the practical application of cloning technologies, these innovations fall short of unveiling the endogenous molecules and mechanisms that an oocyte normally employs to create an embryonic genome. Moreover, enhancing other cellular processes in the cloned embryo could also enhance cloning success.

Identifying the endogenous oocyte factors that promote early cloned embryo development thus remains a valuable objective, for devising ways to improve cloning and for understanding normal development. Obviously, understanding the process of nuclear reprogramming is of widespread interest. Recent advances in identifying exogenous nuclear factors that can promote the establishment of pluripotency in cultured cells have provided new insight into potential reprogramming mechanisms. However, some of the proteins designated as pluripotency or stemness genes are not expressed in the early embryo (Mtango *et al.* 2011), illustrating the importance of identifying the endogenous ooplasmic factors that regulate nuclear programming. It is equally vital to identify the ooplasmic factors that drive other crucial processes, such as energy production, macromolecular processing, cell division, cellular signaling, and maintenance of cell structure in the early embryos. Ooplasmic components that repair the cytoskeleton and cellular architecture, repair the plasma membrane, promote proper pmSCC formation, enable correct mitoses, initiate correct cell cycle transit, and suppress apoptosis may be key for cloned embryogenesis, with parallel roles in the normal embryo. Because the oxidative state of the cell can be compromised by *in vitro* manipulation and this can lead to long-term phenotypic change (Banrezes *et al.* 2011), ooplasmic factors that regulate the oxidative state in clones may also be key. With so many processes potentially contributing to cloned embryogenesis, and the fundamental

interest in understanding these processes in normal embryos, there is clear value in pursuing a systematic approach to identify genes that enable successful cloned embryo development.

We reasoned that identifying endogenous factors in oocytes that drive early development in SCNT embryos would be achievable using an unbiased genome scanning approach that can capture genes contributing quantitatively to SCNT outcome. We combined a mouse recombinant inbred (RI) mapping strategy with MII and GV stage oocyte gene expression data, gene network data and molecular pathway data, and subsequent quantitative analysis of mRNA expression. Using this composite systems genetics approach, we identified three chromosomal intervals that exert genetic control over SCNT embryo preimplantation development and a fourth potential interacting interval. Within these three quantitative trait loci (QTL) we identified a number of candidate genes for which differential expression is significantly associated with SCNT embryonic progression. The strongest genetic candidates correspond to cytoskeletal scaffolding proteins. Additional genes identified in the study encode known pluripotency regulators, transcription factors, and signaling proteins. Collectively, these results provide new insight into the cellular pathways that contribute to the viability of early stage embryos.

Materials and Methods

Mice, embryo culture, and SCNT

Females of 29 BXD recombinant inbred strains were obtained from the Jackson Laboratory (Bar Harbor, Maine) at the age of 8–10 weeks. Females of the C57BL/6, DBA/2J (abbreviated as B6 and D2) and B6D2 F1 hybrid genotypes were also used. B6 stock was obtained from Harlan Sprague-Dawley. D2 stock was obtained from the Jackson Laboratory. B6D2 F1 hybrids were obtained from the National Cancer Institute. MII stage oocytes were obtained by superovulation using 5 IU equine chorionic gonadotropin (eCG) followed 48 hr later by 5 IU human chorionic gonadotropin (hCG). Cloned constructs and parthenogenetically activated embryos were created as described (Chung *et al.* 2006; Han *et al.* 2010a). Clones were prepared using B6D2 F1 cumulus cells as donors for all recipients. SCNT constructs and parthenotes were cultured in MEM α medium supplemented with sodium pyruvate and BSA in a humidified 37° incubator with 5% CO₂ in air as described (Han *et al.* 2010a). This culture medium supports efficiently the development of SCNT embryos (superior to embryo culture formulations) and also supports B6D2 F1 parthenote development (Gao *et al.* 2004).

All studies were approved by the Temple University Institutional Animal Care and Use Committee, consistent with National Institutes of Health (NIH) Guide for the Care and Use of Laboratory Animals, and with AAALAC accreditation.

BXD phenotype analysis

Twelve traits were analyzed using the suite of tools available at <http://GeneNetwork.org> (Andreux *et al.* 2012). We used three of the mapping functions:

1. Interval mapping with the permutation test option was used to identify chromosome intervals and associated genes and markers linked to BXD trait values, and which haplotypes positively and negatively affected the traits. This tool uses a rapid regression method that compares trait values to the known genotype at a marker or the probability of a genotype at given location.
2. Marker regression analysis was used to compute the correlation between genetic variants at loci and phenotypes, and the fraction of strain variance accounted for by each locus. The analysis uses a Pearson product momentum correlation. Data were reported as likelihood ratio statistic (LRS), which provides a measurement of the association between a trait and genetic markers; a significance threshold of $P < 0.05$ is used. The threshold for suggestive LRS values, indicative of potential correlations worthy of further examination, is set at $P < 0.63$. Analyses were performed with and without parental strain data.
3. Composite interval mapping was used to search for possible secondary loci that might be masked by primary loci with genome-wide significant LRS scores. This utility factors out the effect of a primary locus so that any relevant secondary loci can be detected. The GeneNetwork utility uses mouse genome build 37.2.

qRT-PCR and statistical analysis

Quantitative real-time RT-PCR was performed using the Applied Biosystems (ABI, Life Technologies, Carlsbad, CA) Step One Plus system. Primers employed are described in [Supporting Information, Table S1](#). A minimum of three pools of 15–25 oocytes were obtained for each strain. The zona pellucida of MII stage oocytes were removed using acidified Tyrode's buffer (pH 2.5). Total RNA was isolated using the Picopure RNA isolation kit (Life Technologies) according to the manufacturer's recommendation and reverse transcribed using the Superscript III kit (Life Technologies). To provide maximum reproducibility and highest quality data, the PCR analysis was performed without further library amplification. Quantitative real-time PCR was performed using TaqMan gene expression assays according to the ABI protocol. The abundance of each target gene mRNA was normalized to the endogenous *Laptm4b* mRNA for sample-to-sample comparisons. The relative expression ratios among different groups were obtained by the comparative CT method (Livak and Schmittgen 2001) using the Step One software v. 2.1. Pearson correlation coefficients were calculated to evaluate the relationships among the expression levels for the various candidate genes. Gene expression levels were also analyzed for a relationship to the 12 phenotypic traits and to each other.

Results

Study design

Our goal was to identify genes expressed in the oocyte that underlie successful early development in SCNT embryos. Achieving this would advance cloning biology, our understanding of oocyte biology and determinants of oocyte quality, and our understanding of early formative processes in the embryo. The unique capacity of oocytes to reprogram differentiated somatic genomes to an embryonic state implies that unique nuclear reprogramming factors may be expressed in the oocyte. Genes that meet the specific energy needs of nuclear reprogramming could be key facilitators of the process. Genes that code for cytoplasmic components that facilitate protein localization and intracellular signaling could be vital factors to successful cloned embryogenesis. Additionally, genes that support embryo health and viability, inhibit apoptosis, regulate meiotic and cell-cycle progression, and promote homeostasis could participate in determining the success of early cloned embryogenesis and could be sensitive to the dialog between donor genome and ooplasm. In view of the extensive and unique array of ooplasmic factors that could contribute to nuclear reprogramming and early cloned embryo development, we reasoned that an unbiased genome-wide approach was the only plausible means of identifying the major ooplasmic factors that control early SCNT outcome. We therefore adopted a genome scanning approach to identify QTL that contribute to successful development of SCNT constructs to the blastocyst stage. A schematic summary of our overall strategy is provided in Figure 1.

The success of any genome scanning approach is determined in part by the genetic resolution offered by the genetic reference population and by the number of genotypes assayed. Mouse RI strains have been used for >25 years for identifying loci that control many phenotypic traits, and one of the most extensive families of RI mice available is the BXD family. The BXD family of RI strains encompasses ~150 lines (~80 available from the Jackson Laboratory and 70 available from the University of Tennessee Health Science Center) and segregate for ~4.8 million SNPs and 500,000 insertions/deletions, copy number variants, and inversions (Wang *et al.* 2010b) providing a high degree of precision in mapping. Our previous studies revealed a genetic difference between B6, D2, and B6D2 F1 oocytes to support development of SCNT embryos made with B6D2 F1 cumulus cells (Gao *et al.* 2004). Oocytes from B6D2 F1 females support superior preimplantation development and successful term development. Oocytes from B6 females also support preimplantation development but at a lower rate compared to B6D2 F1 oocytes. Oocytes from D2 females do not support efficient clone development beyond the two-cell stage. Thus, the BXD RI panel of mice provided the appropriate genetic resource for quantifying, mapping, and ultimately identifying genes that determine the ability of an oocyte to support early development in SCNT embryos.

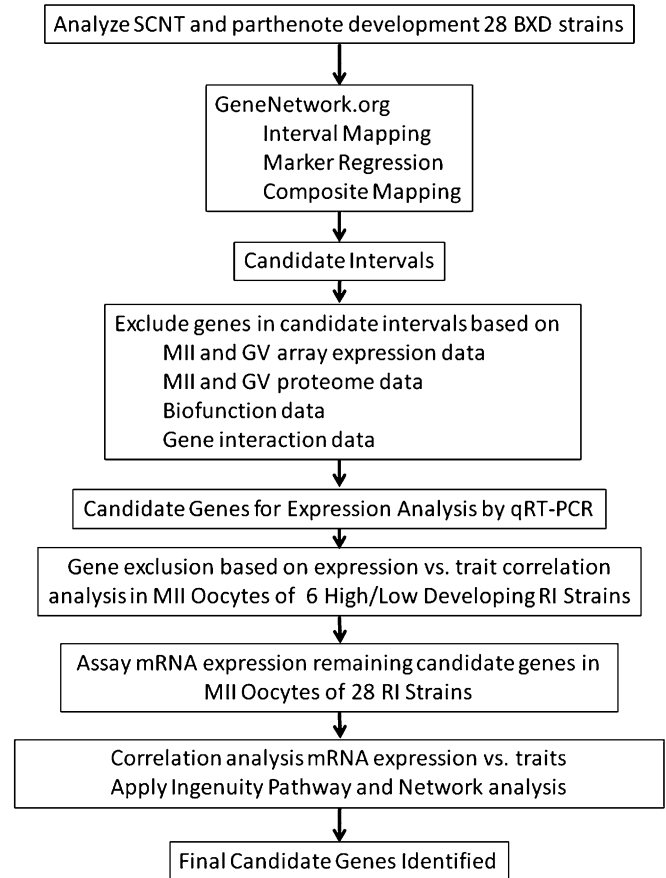


Figure 1 Schematic summary of approach for identifying candidate genes for oocyte factors regulating early development of SCNT embryos. The pathway from phenotype analysis of 28 BXD strains, interval mapping, and then use of diverse sources of published data (Table S5) and qRT-PCR data generated in this study (Tables S6 and S7) to narrow progressively the number of candidate genes from 195 to 26 (Table 3) is shown.

Development was scored for cloned constructs as follows: percentage progression from cloned construct to the two-cell stage, percentage progression from two-cell to four-cell stage, percent progression from four-cell to blastocyst stage, and percentage progression from two-cell to blastocyst stage. The first three measures examine progression through particular windows of development, whereas the progression from two-cell to blastocyst stage examines the overall conversion rate from the time of embryonic genome activation to blastocyst. The transition to the two-cell stage indicates that the embryo had the capacity to form pronuclei (pseudopronuclei in SCNT embryos), replicate DNA and transit the cell cycle, and complete mitotic division successfully. Passage through the first cell cycle is controlled by maternal stores of mRNA, proteins, and other macromolecules, as gene transcription is not required (Mtango *et al.* 2008). The first S phase of mouse embryogenesis is required to establish the ability to transcribe the genome (Latham and Schultz 2001). The two-cell stage is notable for the occurrence of the major transcriptional activation

event, degradation of much of the remaining maternal mRNA, and the transition to reliance on embryonically encoded mRNAs for development. The second S phase in the mouse embryo is required to establish the ability to regulate gene expression, as transcriptional enhancers become necessary (Latham and Schultz 2001). The successful transition from two-cell to four-cell stage indicates successful activation of the embryonic genome. A second major transition in gene expression accompanies progression through the eight-cell stage (Latham *et al.* 1992; Hamatani *et al.* 2006), and as development progresses from four-cell to morula and blastocyst stages, cells in the embryo acquire developmental bias in fate, with innermost cells being more likely to contribute to the inner cell mass and the definitive embryonic lineages, while the outer cells are more likely to contribute to the extraembryonic trophoblast lineage (Chen *et al.* 2010). Conversion from four-cell to blastocyst stage reflects the successful establishment within SCNT embryos of the ability to accomplish such key early developmental benchmarks. By assessing developmental progression through these different developmental windows, insight can be gained concerning genes that may contribute to these key events and which transitions particular genes may be promoting. It is noted that the effects of maternally inherited mRNAs and proteins deposited in the oocyte need not be limited to the first cell cycle. Such factors can execute early actions that have long-term secondary effects (*e.g.*, modulating embryonic gene expression) or can persist during cleavage and exert effects at later stages.

The SCNT developmental values reveal quantitative differences in the overall success of SCNT preimplantation development. The same developmental parameters were calculated for parthenogenetic embryos. The parthenogenetic values provide insight into genetic variations affecting oocyte quality and activation and subsequent embryo cleavage. Parthenotes were chosen because they are subjected to the same chemical activation procedure and are derived from the same pools of oocytes used to generate the cloned embryos. The inclusion of parthenotes in this study also provided an opportunity to observe genetic effects on these processes aside from addressing the genetic control of SCNT outcome. Additionally, the ratios of SCNT:parthenote values were calculated for each of the four parameters. The SCNT:parthenote ratio provides potential insight into effects on processes or nucleus–ooplasmic interactions in SCNT embryos independent of those that affect parthenote development. Essentially, the parthenote data reveal a baseline effect of each genotype on early development, and the SCNT:parthenote ratio provides an indication of genetic variation in cloning outcome that is distinct from this baseline. Collectively, these calculations yielded 12 traits that were subjected to genetic analysis.

Due to cost limitations and labor inherent in determining oocyte strain effects on SCNT outcome, the number of BXD strains that could be tested was limited. We obtained females from 29 of the original BXD strains; one of these

(BXD20) was later reported by the vendor to be genetically contaminated and was excluded from the study. Oocytes from the remaining 28 strains were tested for their ability to support SCNT embryo development and their ability to support parthenogenetic embryo development. We monitored development for cloned constructs and diploid parthenotes prepared with oocytes from these 28 BXD strains, from B6 and D2 strains, and from B6D2 F1 hybrids.

QTL mapping of oocyte traits related to SCNT and parthenogenetic embryo development

To identify QTL associated with cloning outcome, we tested the abilities of oocytes for each BXD strain to support developmental progression in clones in three to five separate replicates. The universal somatic cell donor nucleus was a B6D2 F1 cumulus cell. Between 138 and 307 cloned constructs were prepared for each strain, with a total of 5730 cloned constructs being assayed. An additional 2793 constructs were assayed for the B6, D2, and B6D2 F1 genotypes, for a total of >8500 cloned constructs assayed. A total of 2612 parthenotes were tested for the BXD strains and 472 for the B6, D2, and B6D2 F1 genotypes.

For SCNT embryos, most BXD strains supported development to the two-cell stage, some even exceeding the value for B6D2 F1 oocytes, but some strains supported two-cell development very poorly (BXD12, BXD33, BXD42) (Table 1). Progression from two-cell to four-cell stages was >50% for eight strains, between 20 and 50% for nine strains, and < 20% for 11 strains. Progression from the two-cell stage to blastocyst stage was >20% for only two strains (BXD11 and BXD27), which is comparable to rates of 20.9 and 27.4% for the B6 and B6D2 F1 genotypes. This suggests that multiple loci are likely to control this overall transition from first cleavage to blastocyst formation. For progression from the four-cell stage to blastocyst stage, seven strains supported development at >30%, comparable to 37.9 and 36.3% for B6 and B6D2 F1 oocytes, indicating that a small number of loci may control the four-cell to blastocyst transition.

Parthenogenetic development proceeded for most strains, but some strains displayed severely reduced rates of activation and progression to the two-cell stage (BXD12, BXD33, BXD42) and/or reduced development beyond the two-cell or four-cell stages (Table 1). The D2 strain displayed efficient parthenogenetic development to the two-cell stage but restricted development thereafter. These data thus reveal significant genetic effects on oocyte activation and cleavage that are likely independent of the SCNT procedure, but that nevertheless contribute to the overall outcome of the procedure.

The data from Table \1 were subjected to interval mapping and marker regression analysis using the tools at GeneNetwork.org. Analysis of the results for the four SCNT embryo development traits yielded a major controlling locus on chromosome (chr) 17, and additional loci on chr 1 and 4 (Table 2). The region on chr 17 (map position 69.1492–71.10156 Mb) was returned by trait analysis with a significant LRS value for both the two-cell to four-cell conversion

Table 1 Percentage developmental progression of cloned and parthenogenetic embryos prepared with eggs from different strains

BXD Strain																
SCNT	1	2	5	6	8	9	11	12	13	14	15	16	18	19	21	22
Two cell/construct	59.6	75.4	77.4	38.2	80.7	97.7	79.8	11.6	57.1	71.2	80.6	82	66	84.4	85.2	77.4
Four cell/two cell	0	20.5	52.3	1.2	28.1	15	64.2	15.3	53.9	17.4	4	15.2	42.1	49.7	14.7	54.5
Blastocyst/two cell	0	7.6	11.9	1.2	6.8	4.5	27.5	0	16.5	5.7	0	0	10.4	4.6	4.5	11
Blastocyst/four cell	0	29.5	17.9	25	16.8	31.9	43	0	34.5	27.3	0	0	25.4	9.1	31.3	19.3
	27	28	29	31	32	33	34	36	38	39	40	42	B6	D2	F1	
Two cell/construct	51	82.1	78.5	43.8	70.1	15.6	84.8	86.3	56.9	72.4	93.5	23.1	68.3	64.7	87.3	
Four cell/two cell	59	29.8	10.7	7.3	50.6	0	48.9	37.2	45.8	3	66	39.2	53.6	43	66	
Blastocyst/two cell	23.7	8.7	0.9	5.2	8	0	13.9	17.5	4.3	1.2	16.1	7	20.9	0	27.4	
Blastocyst/four cell	37.9	32.9	5.8	55.6	21.5	0	26.6	54.4	6.9	27.8	24.2	10.7	37.9	0	36.3	
Parthenote	1	2	5	6	8	9	11	12	13	14	15	16	18	19	21	22
Two cell/activated	85.4	97.4	91.9	98.2	91.7	97.7	95.7	22.7	97.4	78.4	97.5	99.2	80.2	100	98.6	95.7
Four cell/two cell	5.3	100	59.3	83.1	52.9	86.4	95	79.5	77.8	55	49.2	9.4	73.6	81.4	79.3	78
Blastocyst/two cell	0	91.5	5.6	0	2.5	38.8	83.6	7.3	38.7	11.7	33.7	0	40.9	18.8	57.5	12.6
Blastocyst/four cell	0	91.5	7.9	6.1	3.6	44.6	88.8	7.5	46.9	16.7	62.8	0	54.8	23.4	72	16.4
	27	28	29	31	32	33	34	36	38	39	40	42	B6	D2	F1	
Two cell/construct	66.7	97.5	91.3	95.1	94.3	19.4	100	90.1	66.3	84.4	95.7	39.6	84	72.6	100	
Four cell/two cell	100	97.1	31.7	85.2	61.3	46.7	89.8	60.1	13.5	84.6	100	80	100	59	99.6	
Blastocyst/two cell	77.1	64.7	3.3	39.9	22.5	12.5	48.6	14.7	3.8	61.5	74.5	8.3	36.8	2.1	72.2	
Blastocyst/four cell	77.1	66.4	6.7	46.7	39.5	17	54.7	26.3	35	73.8	74.5	8.3	36.8	2.5	72.6	
SCNT:parthenote	1	2	5	6	8	9	11	12	13	14	15	16	18	19	21	22
Two cell/construct	69.8	77.5	84.2	38.9	88	100	83.4	50.9	58.7	90.8	82.6	82.7	82.3	84.4	86.4	80.9
Four cell/two cell	0	20.5	88.2	1.4	53.2	17.4	67.5	19.2	69.3	31.7	8	163	57.2	61.1	18.6	69.9
Blastocyst/two cell	0	8.3	215	0	273	11.5	32.9	0	42.7	48.9	0	0	25.4	24.7	7.9	87.7
Blastocyst/four cell	0	32.3	227	408	469	71.4	48.4	0	73.5	164	0	0	46.2	39.1	43.4	118
	27	28	29	31	32	33	34	36	38	39	40	42	B6	D2	F1	
Two cell/construct	76.5	84.2	86.1	46.1	74.3	80.3	84.8	95.7	85.8	85.9	97.7	58.4	81.3	89	87.3	
Four cell/two cell	59	30.7	33.7	8.6	82.5	0	54.4	61.9	339	3.6	66	49.1	53.6	72.9	66.3	
Blastocyst/two cell	30.7	13.4	28.9	13	35.7	0	28.6	119	115	2	21.6	84.5	56.8	0	37.9	
Blastocyst/four cell	49.2	49.6	87.7	119	54.5	0	48.7	207	19.8	37.7	32.5	129	103	0	49.9	

Values show the percentage progression from SCNT construct to two-cell stage, from two-cell to four-cell stage, from two-cell stage to blastocyst stage, and from four-cell stage to blastocyst. Development was scored for SCNT embryos and for parthenotes made with oocytes from the 28 strains. The ratio of SCNT:parthenote development was also calculated for each strain.

and the two-cell to blastocyst conversion, when the BXD data were analyzed without including parental strain data, and displayed a suggestive LRS value with parental strain data included. A second region with a significant LRS value was seen on chr 4 (map position 13.03102–13.76499 Mb) for the two-cell to four-cell conversion trait without parental strain data and displayed a suggestive LRS value when parental strain data were included. For both the chr 4 and chr 17 regions, a D2 haplotype was positively associated with SCNT development. A third region showing a significant LRS value, seen with the transition from the two-cell to blastocyst stage, was observed for chr 1 (map position 40.99094–42.21652 Mb) when parental strain data were included and was just below the significance threshold (but retained a suggestive LRS value) without parental strain data included. For the chr 1 region, a B6 haplotype was positively associated with SCNT embryo development. Each of these regions was flanked by additional markers that displayed suggestive LRS values.

The above three regions on chr 1, 4, and 17 were the only regions to achieve statistical significance in any of the 12 traits assayed. An additional region on chr 9 displayed suggestive LRS values for three of the SCNT traits and also

displayed suggestive LRS values for parthenogenetic development from two- or four-cell stage to blastocyst, accompanied by a region on distal chr 13 (Table S2). Additional suggestive LRS values were obtained for other regions on chr 6, 8, 13, and 16 when analyzing the SCNT:parthenote ratios (Table S3). To test whether any of these regions displayed significant interactions with the regions on chr 1, 4, and 17, we applied composite interval mapping to the SCNT trait data with or without parental strain data included (Table S4). Without parental strain data included, we identified two small regions on chr 6 that yielded suggestive LRS values for interactions with markers in the chr 17 region when examining the two-cell to blastocyst conversion trait without parental strain data. With parental strain data included, the same trait yielded markers on chr 7 and 11 with suggestive LRS values for interactions with markers in the chr 1 region.

Overall, these data indicate that there is a primary QTL on mouse chr 17 that is correlated with multiple trait measures of preimplantation SCNT developmental progression, that additional intervals on chr 1 and 4 display significant LRS values for associations with SCNT development, and that other interacting loci (particularly the ones on chr 6) may

Table 2 Marker regression analysis and interval mapping of cloned embryo development

With parents Four cell/two cell					Without parents Four cell/two cell				
Chr	Mb	Mb	Haplotype incr. trait	LRS	Chr	Mb	Mb	Haplotype incr. trait	LRS
1	40.990937	42.216521	B6	10.723	4	6.820702	11.507152	D2	12.98
4	6.820702	11.507152	D2	11.606	4	13.031015	13.764991	D2	19.826*
4	13.031015	13.764991	D2	17.548	17	66.785539	68.482569	D2	13.914
17	66.785539	68.482569	D2	11.486	17	69.149197	71.101564	D2	20.652*
17	69.149197	71.101564	D2	17.121	17	71.350424	72.001676	D2	13.914
17	71.350424	72.001676	D2	11.486	17	76.561294		D2	11.731
	Suggestive LRS			10.35		Suggestive LRS			11.03
	Significant			18.29		Significant			19.49
	Highly significant			22.66		Highly significant			24.69
Blastocyst/two cell					Blastocyst/two cell				
Chr	Mb	Mb	Haplotype incr. trait	LRS	Chr	Mb	Mb	Haplotype incr. trait	LRS
1	29.231425	30.978257	B6	13.63	1	29.231425	30.978257	B6	11.149
1	38.079087	39.05313	B6	12.315	1	39.578771		B6	10.027
1	39.578771		B6	12.583	1	40.990937	42.216521	B6	15.158
1	40.990937	42.216521	B6	17.992*	4	13.031015	13.764991	D2	13.282
9	59.835172	59.934576	B6	10.33	17	66.785539	68.482569	D2	13.946
9	72.030418	72.952358	B6	11.781	17	69.149197	71.101564	D2	18.806*
9	73.368885	76.983761	B6	10.331	17	71.350424	72.001676	D2	13.946
9	77.217283	79.902981	B6	11.725					
9	79.991491	81.159484	B6	10.061					
17	69.149197	71.101564	D2	9.997					
	Suggestive LRS			9.87		Suggestive LRS			9.94
	Significant			16.2		Significant			16.02
	Highly significant			19.65		Highly significant			19.51
Blastocyst/two cell					Blastocyst/two cell				
Chr	Mb	Mb	Haplotype Incr. Trait	LRS	Chr	Mb	Mb	Haplotype Incr. Trait	LRS
1	29.231425	30.978257	B6	11.227	1	40.990937	42.216521	B6	13.428
1	40.990937	42.216521	B6	16.274	9	69.810185	70.880253	B6	11.217
9	68.191194	69.455899	B6	12.427	9	71.331037	71.798886	B6	10.603
9	69.810185	70.880253	B6	13.589	9	72.030418	72.952358	B6	10.433
9	71.331037	71.798886	B6	12.973	9	73.368885	76.983761	B6	11.109
9	72.030418	72.952358	B6	12.739	9	79.991491	81.159484	B6	11.851
9	73.368885	76.983761	B6	13.526					
9	77.217283	79.902981	B6	12.255					
9	79.991491	81.159484	B6	14.437					
	Suggestive LRS			10.23		Suggestive LRS			10.42
	Significant			16.66		Significant			16.96
	Highly Significant			20.13		Highly Significant			19.67

*, significant correlation of region with trait.

also exist. Additional genotypes would need to be tested to provide a robust test of the relevance of these other loci to SCNT embryo development; hence these loci were not pursued further in this study.

It is noted that the BXD strains and the B6 and B6D2 F1 mice employed in these analyses encompass different B6 substrains; BXD mice are based on B6J substrain while Harlan B6 and NCI B6D2 F1 mice are based on the B6N substrain. However, the LRS intervals on chr 4 and 17 were identified as significant using the BXD strain data without the parental data and were scored as suggestive with the parental data added, while the chr 1 locus was significant with parental data and scored as suggestive without the

parental data included. Hence, the identification of these three candidate intervals was unlikely to be affected by minor genetic variation between the B6N and B6J substrains. It is also noted that, while genetic polymorphisms exist between these substrains and can affect phenotype, the two substrains are quite close genetically. One study reported just 11 of 1446 SNPs variant between B6J and B6N (Mekada *et al.* 2009), and another reported just 12 of 1449 SNPs as variant (Zurita *et al.* 2011). Another study reported the two substrains differ in 12 of 342 microsatellite markers surveyed (Bothe *et al.* 2004). Genome sequencing revealed just 150 SNPs between the two substrains (Bryant 2011) and commercial vendors advertise 95–128 diagnostic SNP panels for discriminating

Table 3 Number of genes evaluated and included in further detailed study by chromosome region

Chr	Region and LRS significance	No. genes	No. tested on 6 BXD strains	No. tested on 28 BXD strains
1	Significant	1	0	0
	Suggestive	47	11	9
4	Significant	3	1	1
	Suggestive	57	10	7
17	Significant	13	3	3
	Suggestive	74	11	6
Total		195	36	26

B6 substrains. These studies also reveal that the different B6 substrains are closely related to each other. By contrast, the B6 and D2 strains are genetically distant from one another (Taylor 1972). We observed little difference in mRNA expression ratios for three mRNAs selected to compare results for oocytes from females obtained from the Jackson Laboratory and Harlan Sprague-Dawley (data not shown). The dramatic difference between B6 and D2 inbred genotypes in cloning outcome would make an effect of substrain genetic background on the QTL mapping result unlikely, accounting for the emergence of the candidate loci with and without parental strain data included in the analysis.

Initial evaluation of candidate genes

The combined three significant LRS regions and the flanking suggestive regions collectively encompassed 195 genes. Our next goal was to identify a subset of these genes to be examined in detail for association with oocyte cloning phenotype. Using a systems genetics approach, QTL mapping can be combined with other data (gene expression, polymorphisms, gene ontology) to achieve an identification of specific genes or combinations of genes that may contribute to a specific phenotype, in this case the ability of the oocyte to support early SCNT embryo development. We incorporated available transcriptome profiling data for B6, D2, and B6D2 F1 hybrid MII and germinal vesicle stage oocytes, as well as knowledge of biological function and cellular compartment localization and oocyte proteome data (Wang *et al.* 2010a), to narrow the lists of candidate genes for further study. Candidate genes were further scrutinized on the basis of sequential qRT-PCR expression analyses. The combination of these additional data for individual gene characteristics narrowed markedly the array of candidate genes. The presence and numbers of SNPs upstream of the 5'-UTR and within protein-coding regions were also noted, as polymorphisms within the coding regions could affect a trait independent of gene expression level. From the three candidate intervals defined by the significant LRS values and flanking suggestive LRS value intervals, we identified 36 genes for detailed study (Table 3).

A detailed summary of the gene characteristics and expression data supporting our focus on this set of 36 genes is given in Table S5. Because the <http://GeneNetwork.org> application uses genome build 37.2, Table S5 incorporates map locations for this build as well as build 38; assignment

to intervals with significant LRS values was based on build 37.2 positions, for consistency with the <http://GeneNetwork.org> application. We first characterized genes on the basis of detection and maximum raw intensity values observed with Affymetrix MOE430v2 arrays corresponding to MII stage oocytes from B6, D2, and B6D2 F1 strains (note that these arrays employed mice from the Jackson laboratory). The array data set (unpublished) incorporated four replicate arrays for each strain for the MII and germinal vesicle stages. Array data displayed robust quality control parameters consistent with previously reported arrays for oocyte samples from mouse and other species (Pan *et al.* 2005; Lee *et al.* 2008). Genes with no detected expression on the MII array were excluded from further consideration. The remaining genes were evaluated as candidates for further study on the basis of maximum array average intensity values, array fold changes between strains, qRT-PCR expression ratios between B6, D2, and B6D2 F1 oocytes, biological functions, and cellular compartmentalization. Genes meeting a combination of at least 500 maximum raw intensity value on array, at least twofold change on array, and at least 10% change in qRT-PCR among oocyte samples for B6, D2, and B6D2F1 genotypes were included for further study. For genes showing weak or no expression in MII stage oocytes, germinal vesicle stage arrays were consulted to account for possible protein contributions to MII oocyte phenotypes, where the mRNAs might be degraded during oocyte maturation. Pseudogenes were excluded. Absence of functional annotation was also a criterion for excluding genes lying outside of the intervals with significant LRS values. The miRNA genes were excluded due to the limited role of miRNAs in oocytes and embryos (Svoboda 2010). Genes encoding noncoding RNAs outside of the significant LRS intervals and with no probe coverage on the array were not examined. Genes encoding secreted proteins, components of the extracellular matrix, mitochondrial proteins, cell adhesion proteins, and DNA repair proteins were deemed of lower priority. Germinal vesicle and MII oocyte proteome data were also examined to identify genes with expression at the protein level. Most genes excluded from detailed study were excluded on the basis of a combination of criteria.

Highest priority for further study was assigned to genes in the regions with significant LRS values. The chr 1 region encompassed one pseudogene. This region was flanked by another pseudogene and one noncoding RNA gene for which

expression was not detected in oocytes by qRT-PCR. Additional chr 1 genes centromeric to this region were included in the analysis, as described below. The chr 4 region encompassed two pseudogenes and a single protein-coding gene, *Runx1t1*. The chr 17 region encompassed 13 genes. Four of these were pseudogenes, one was a noncoding RNA poorly expressed on the array, and three were uncharacterized sequences or characterized as predicted protein coding gene. Two genes were excluded on the basis of a weak signal and small expression differences on arrays. The remaining chr 17 genes included in the study were *Epb4.1l3*, *Zfp161*, and *Dlgap1* (Table 3 and Table S5).

Other genes within the flanking suggestive intervals on chr 1, 4, and 17 were evaluated for further study. For the chr 1 region, an immediately flanking noncoding RNA (*4930448I06Rik*) with no reported expression in oocytes or embryos was examined by qRT-PCR with no detected expression and was therefore excluded. Eleven other genes centromeric to the significance interval were examined, including genes immediately adjacent to the noncoding RNA gene. For the chr 4 interval, an adjacent long noncoding RNA gene (*Gm11818*) was examined, but excluded due to little expression difference between B6, D2, and B6D2 F1 oocytes by qRT-PCR. Nine additional candidates were selected from this flanking suggestive interval. For the chr 17 flanking suggestive intervals, 11 genes were selected for detailed study. Two genes (*Myl12a* and *Myl12b*) related to myosin contractility and cellular shape change were not included in the initial analysis due to uncertain functional relevance and limited difference in expression on arrays; one of these (*Myl12a*) was subsequently tested on the B6, D2, and B6D2 F1 genotypes by qRT-PCR (Table S5) but was not subjected to full analysis. Some genes located in the suggestive chr 17 intervals were excluded from further consideration because of reported cell type-specific expression and functions. One additional gene (*Memo1*) on chr 17 related to cell motility was excluded on the basis of its reported function. Taking into account the available array data, and the other data summarized in Table S5, including data obtained by qRT-PCR for expression B6, D2, and B6D2 F1 oocytes, we incorporated an additional 32 genes from these chr 1, 4, and 17 suggestive intervals, for a total of 36 genes studied in detail (Table 3 and Table S5, green highlight in column 1).

These 36 genes were first tested for differences in expression between three BXD strains that displayed maximum developmental outcomes (BXD11, BXD22, and BXD40) and three that displayed minimum developmental outcomes (BXD1, BXD16, and BXD29) for cloned embryo preimplantation development. Limiting our initial analysis to genotypes at the two extremes of phenotype distribution minimized the costs associated with collecting sufficient numbers of MII stage oocytes needed for qRT-PCR without benefit of mRNA amplification. Of these 36 genes tested (Table S6), 10 were excluded from further study because they showed either no or limited correlations with the four SCNT traits monitored.

Four of the remaining 26 genes failed to display a strong correlation with the phenotypes of these six BXD strains, but were retained for further study because they encode biological functions deemed of high potential relevance or because they lie within or very near the intervals displaying significant LRS values. This yielded a final list of 26 genes for analysis on the entire set of 28 BXD strains used in our analysis (Table 3).

Single gene expression correlations with SCNT developmental traits for Chr 1, 4, 17 regions

To identify those genes most likely to contribute to cloning outcome, our next goal was to identify from among this list of 26 candidates, the genes that manifested significant correlations between expression and phenotype. We evaluated correlations between gene expression and the SCNT embryo and SCNT:parthenote developmental phenotypes for the 28 BXD lines (Table S7). We initially excluded B6, D2, and B6D2 F1 genotype expression data, and then examined the effects of including these genotypes. We also compared associations with SCNT traits alone and associations seen in the SCNT:parthenote ratios. This provided a means of detecting relationships that were specific to SCNT development. Enhancement or acquisition of a significant association revealed in the SCNT:parthenote values relative to SCNT trait values indicates a partial component of the SCNT phenotype that is specific to SCNT biology. Disappearance of an association indicates a predominant effect that is not specific to SCNT biology. An association seen in both SCNT and SCNT:parthenote traits indicates an association with a large SCNT-specific component. Because such associations are quantitative and reflect additive components, effects related specifically to SCNT development could be seen even without significant associations in parthenotes.

The chr 1 interval displaying a significant LRS value encompasses one pseudogene and is adjacent to another pseudogene and a noncoding RNA gene (*4930448I06Rik*, no expression detected). These genes were excluded from further consideration. Immediately centromeric to this region, however, are two genes, *Mfsd9* and *Tmem182*. The *Tmem182* gene, which lies immediately adjacent to the significance interval, displayed highest expression in B6 oocytes (Table 4). The expression of *Tmem182* was strongly and negatively correlated with SCNT embryo development for three of the SCNT traits scored (two-cell conversion to four-cell and blastocyst, and four-cell conversion to blastocyst) (Table 4 and Table S7), which is at odds with the positive effect of the B6 haplotype in this region with outcome. With B6, D2, and B6D2 F1 genotypes included, the *Tmem182* association retained significance only for the conversion from four cell to blastocyst. No associations were seen for SCNT:parthenote developmental ratios, indicating that the associations seen with SCNT embryos were largely not specific for SCNT development. The *Mfsd9* mRNA was also expressed more highly in B6 than D2 oocytes, but to a lesser degree. *Mfsd9* expression displayed a single significant negative correlation with

Table 4 Summary of correlations of gene expression and traits assayed using the panel of 28 BXD strains

Gene	Chr	SCNT				SCNT:Parthenote				Parthenotes				MII Expr. Ratio B6:D2:F1
		2C/ 1C	4C/ 2C	BL/ 2C	BL/ 4C	2C/ 1C	4C/ 2C	BL/ 2C	BL/ 4C	2C/ 1C	4C/ 2C	BL/ 2C	BL/ 4C	
Genes in or near significant LRS intervals														
Mfsd9	1			(\)		X	(X)	(X)		(\)				1:0.71:0.97
Tmem182	1		(\)	(\)	(X)					(X)	(X)	(X)		1:0.32:0.49
Runx1t1	4				(\)*	/		(X)						1:1.09:1.37
Arhgap28	17		(X)	(X)	(X)	(X)	(\)							1:0.07:0.77
Epb4.1l3	17		X	X				(X)	(X)					1:2.6:1.98
Dlgap1	17		(\)	/,(\)			(\)			/				1:0.15:0.61
Tgif1	17			(X)		\	X			(X)	(X)	(X)		1:1.28:0.92
Other genes in suggestive LRS intervals														
Phf3	1		(/)			(X)		X		X				1:0.95:0.99
Txnac9	1		(X)	(X)	(X)			X		(X)	(X)	(X)		1:5.23:3.12
Eif5b	1		(X)	(X)	(X)	(\)				(X)	(X)	(X)		1:1.23:1.25
Aff3	1				(X)					(X)	(\)			1:1.7:1.7
Pdcl3	1		\	\				(\)	X		\			1:0.69:1.01
Tbc1d8	1				(X)									1:1.11:1.08
D1Bwg0212e	1			(\)	(X)			X		(X)	(X)	(X)		1:0.82:0.89
Car8	4		(X)	(X)		(X)		X				(\)		1:0.14:0.61
Rab2a	4		/	/										1:0.87:1.01
Chd7	4		/			/		(X)	(X)					1:1.09:1.39
Asph	4	X				X	X	X		(X)	(X)	(\)		1:1.26:1.35
Ccne2	4	(X)			(X)		X	X		(X)	(X)	(X)	(/)	1:2.36:1.37
Dpy19l4	4									/				1:1.15:1.02
Esrp1	4		/	/		/	X	\						1:0.86:0.89
Smchd1	17	/	(X)	(X)	(X)	(\)				(\)				1:0.91:1.54
Ndc80	17	X	(X)	(X)	(X)			(X)		X	(X)			1:0.23:0.57
Ypel5	17		X	X			X	X						1:1.39:1.26
Lclat1	17	(/)			(X)		X	X		(X)	(X)	(X)	(X)	1:1.51:1.15
Spast	17		(X)	(X)	(\)					/				1:0.69:1.21

/, significant association with trait with B6, D2 and B6D2F1 data included; \, significant association with trait without B6, D2 and B6D2F1 data included; X, significant association with trait with and without B6, D2, and B6D2F1 data included; (), negative correlation of expression with developmental trait; *, marginal significance with parental data included.

SCNT embryo progression from the four-cell stage to blastocyst. With B6, D2, and B6D2 F1 genotypes included this association fell below the level of significance. With the SCNT:parthenote ratio, however, *Mfsd9* gene expression displayed a strong positive association with development from the two-cell to four-cell stage and then strong negative associations with development from the two-cell and four-cell stages to blastocyst, both with and without B6, D2, and B6D2 F1 genotypes included. Thus, of these two genes, only *Mfsd9* displayed a positive association between expression and any developmental trait measured, consistent with the positive effect of the *B6* haplotype, and this was for early progression to the four-cell stage and specific to cloned embryo development. This effect seems to overcome a negative effect seen for parthenotes. The later negative SCNT-specific association, however, indicates stage specificity to the SCNT-specific component.

The chr 4 interval having a significant LRS value contains a single gene, *Runx1t1*. There was not a strong difference in expression between B6 and D2 oocytes, and the mRNA was only modestly elevated in F1 oocytes (Table 4). *Runx1t1* expression displayed a significant negative association with progression from the four-cell to blastocyst stage for SCNT

and SCNT:parthenote traits without B6, D2, and B6D2 F1 genotypes included (Table 4 and Table S7). With B6, D2, and B6D2 F1 genotypes included, *Runx1t1* expression displayed a marginally significant negative association with SCNT embryo development from the four-cell to blastocyst stage ($P = 0.0639$), a significant positive association with the SCNT:parthenote two-cell to four-cell development and a negative association with SCNT:parthenote four-cell to blastocyst development. Thus, there was an enhancement of associations in the SCNT:parthenote traits, indicating a significant negative association specific to cloning.

The chr 17 interval with a significant LRS value encompasses two genes analyzed on all 28 strains (*Epb4.1l3* and *Dlgap1*); a third gene (*Zfp161*) failed to show significant associations with the first 6 BXD lines and so was excluded from further study (Table S6). This region is flanked by an immediately distal gene (*Tgif1*) and a more centromeric gene (*Arhgap28*), both of which were analyzed. The *Epb4.1l3* gene displayed a much higher level of expression in D2 oocytes than either B6 or B6D2 F1 oocytes, and B6D2 F1 oocytes expressed this mRNA nearly twice as highly as B6 oocytes. The *Dlgap1* and *Arhgap28* mRNAs were greatly reduced in D2 oocytes and more modestly reduced in B6D2 F1 oocytes. The

Epb4.1l3 gene displayed significant positive associations of expression with SCNT development from two-cell stage to four-cell and blastocyst stages with and without B6, D2, and B6D2 F1 genotypes included (Table 4 and Table S7), consistent with the elevated expression in D2 oocytes and the positive effect of the D2 haplotype on SCNT traits (Table 2). Despite the positive association with SCNT traits, a negative association was seen between *Epb4.1l3* and the SCNT:parthenote four-cell to blastocyst development, with or without B6, D2, and B6D2 F1 genotypes included. This was not seen in the SCNT traits, and thus was a specific component related to cloned embryo biology. The *Dlgap1* gene displayed several negative expression associations with SCNT two-cell to four-cell and blastocyst development. These were not apparent for the SCNT:parthenote traits, but a significant negative association was seen for SCNT:parthenote two-cell to blastocyst conversion without B6, D2, and B6D2 F1 genotypes included. These associations were consistent with lower expression in D2 oocytes and the positive effect of D2 haplotype on development. *Dlgap1* displayed a positive association between expression and SCNT two-cell to blastocyst conversion with B6, D2, and B6D2 F1 genotypes included, but this was also absent with the SCNT:parthenote traits. *Arhgap28* displayed strong, significant negative associations of expression with the SCNT two-cell conversion to four-cell and blastocyst and four-cell to blastocyst conversion both with and without B6, D2, and B6D2 F1 genotypes included. This was also evident in the two-cell to four-cell SCNT:parthenote developmental values with and without B6, D2, and B6D2 F1 genotypes, indicating that this association may be largely specific to cloned embryos. This association is consistent with the low expression in D2 oocytes and the positive effect of the D2 haplotype for this region (Table 4 and Table S7). *Tgif1* expression displayed a significant negative association of expression with SCNT four-cell to blastocyst conversion and a positive association with SCNT:parthenote two-cell to four-cell conversion rate, both with and without B6, D2, and B6D2 F1 genotypes included, and a positive association with the SCNT:parthenote zygote to two-cell conversion rate indicating a SCNT-specific relationship early during cleavage (Table 4 and Table S7). Thus, of the genes within or near the chr 17 significance interval, *Epb4.1l3*, *Dlgap1*, and *Arhgap28* display the most extensive relationships between expression and developmental outcomes.

In addition to genes within the intervals with significant LRS values (and those immediately flanking the significance region on chr 1), some genes within the flanking suggestive intervals displayed significant associations of expression with one or more of the SCNT and SCNT:parthenote traits (Table 4 and Table S7). Most prominent among these were chr 17 genes *Ndc80* and *Smchd1*, and the transcriptionally coupled chr 1 genes *Txndc9* and *Eif5b*, each negatively correlated with three to four SCNT traits, with and without B6, D2, and B6D2 F1 genotypes included.

The negative associations seen for *Txndc9* and *Eif5b* are consistent with higher expression in D2 oocytes but positive

effects of the B6 haplotype at this region. *Txndc9* and *Eif5b* were generally coregulated as expected for genes that share regulatory elements, having strong associations of expression with three of the SCNT traits, but for the SCNT:parthenote traits these associations were not apparent, except for *Txndc9* for the four-cell to blastocyst conversion and *Eif5b* for the two-cell to four-cell conversion. The associations between expression and development for these two genes were thus not specific to cloned embryogenesis.

The negative association seen for chr 17 gene *Ndc80* expression is consistent with the lower expression level in D2 oocytes and the positive effect of the D2 haplotype at this region. Conservation of this relationship in the SCNT:parthenote two-cell to blastocyst conversion trait indicates a specific component of cloned embryo development. A similar agreement is not as apparent for *Smchd1*, for which expression was only slightly different between strains. A significant negative association of *Smchd1* expression was seen for the SCNT:parthenote two-cell to four-cell conversion trait without B6, D2, and B6D2 F1 genotypes included. Although parthenote development from two-cell to four-cell stage also displayed this association, its persistence at the level of SCNT:parthenote ratio indicates a specific negative contribution to clone development.

The chr 1 gene *D1Bwg0212e* (also known as *C2orf29*) displayed a significant negative association of expression with SCNT two-cell to blastocyst conversion without B6, D2, and B6D2 F1 genotypes included and with SCNT four-cell to blastocyst conversion, both with and without B6, D2, and B6D2 F1 genotypes included. A positive association of expression was acquired, however, for SCNT:parthenote two-cell to blastocyst conversion with B6, D2, and B6D2 F1 genotypes included, indicating a potential beneficial effect specific to cloned embryos. *D1Bwg0212e* expression was slightly elevated in B6 compared to D2 oocytes, potentially contributing to a positive effect of the B6 haplotype. The chr 1 gene *Phf3* displayed no significant difference in expression between B6, D2, and B6D2 F1 oocytes, a single negative association for the two-cell to four-cell SCNT conversion, and conflicting associations among the SCNT:parthenote traits indicating possible stage specific effects in cloned embryos.

The chr 4 gene *Chd7* displayed elevated expression in B6D2 F1 oocytes, plus a positive association of expression with SCNT two-cell to four-cell conversion with B6, D2, and B6D2 F1 genotypes included. For the SCNT:parthenote traits, *Chd7* mRNA expression was positively associated with formation of two-cell embryos. Thereafter, it was negatively associated with SCNT:parthenote traits of two-cell and four-cell conversions to blastocyst stage with and without B6, D2, and B6D2 F1 genotypes included, indicating a significant SCNT-specific function in later cleavage. The chr 4 gene *Ccne2* displayed significant negative associations of expression with the two SCNT traits of zygote to two-cell and four-cell to blastocyst conversion, at odds with the higher expression value for D2 oocytes. However, *Ccne2* displayed positive

associations with the SCNT:parthenote traits for two-cell conversion to four-cell and blastocyst, with and without B6, D2, and B6D2 F1 genotypes included, indicating an SCNT-specific component of its actions. Another chr 4 gene, *Car8*, displayed lower expression in D2 oocytes plus significant negative associations of expression with the two SCNT traits of two-cell to four-cell and two-cell to blastocyst conversion with and without B6, D2, and B6D2 F1 genotypes included. The negative association was reiterated for SCNT:parthenote ratio of two-cell to four-cell conversion with and without B6, D2, and B6D2 F1 genotypes included. A positive association for *Car8* expression was seen for SCNT:parthenote four-cell to blastocyst conversion, indicating a second SCNT-specific component to its effect. *Asph* displayed elevated expression in D2 and F1 oocytes, positive associations with SCNT:parthenote ratios for development, and negative associations with parthenote development.

Another chr 17 gene, *Ypel5*, displayed a slightly increased expression value for D2 compared to B6 oocytes, along with positive associations of expression with two-cell to four-cell and two-cell to blastocyst conversions for both SCNT and SCNT:parthenote traits, both with and without B6, D2, and B6D2 F1 genotypes included. The effects of *Ypel5* thus appeared to have a strong SCNT-specific component independent of more general effects occurring in parthenotes (none observed). The *Spast* gene displayed modestly reduced expression in D2 compared to B6 oocytes, along with significant negative associations with two-cell to four-cell and two-cell to blastocyst SCNT conversions, with and without B6, D2, and B6D2 F1 genotypes, an association with four-cell to blastocyst conversion without B6, D2, and B6D2 F1 genotypes included, but no associations with SCNT:parthenote traits, indicating that its effects are relatively nonspecific for SCNT development.

Single gene correlations between expression and parthenote development

Processes shared between SCNT embryos and parthenotes may affect SCNT developmental characteristics. The data for parthenote development provide an opportunity to delineate further gene expression effects that are attributable specifically to nuclear reprogramming and SCNT development and an opportunity to dissect effects on oocyte activation and development in the absence of paternally derived chromosomes. With respect to genes associated with the intervals having significant LRS values, gene expression associations for *Runx1t1*, *Epb4.1l3*, *Mfsd9*, and *Arhgap28* were generally not consistently seen in the parthenote traits, whereas associations observed for *Tmem182* and *Tgif1* were seen for parthenotes, with and without B6, D2, and B6D2 F1 genotypes included (Table 4 and Table S8). There was a negative association of *Epb4.1l3* expression with parthenote conversion to the two-cell stage. Many of the effects seen for *Smchd1*, *Ypel5*, *Dlgap1*, *Spast*, and two of the *Ndc80* associations were also not seen extensively for parthenotes, with or without B6, D2, and B6D2 F1 genotypes included.

Effects seen for chr1 genes *Eif5b*, *Txndc9*, and *D1Bwg0212e* were also present for parthenotes, and thus were not specific to SCNT embryos. With respect to unique associations of gene expression with parthenote development, the most prominent effect was seen for *Lclat1*, having significant negative associations with all four parthenote traits, but also for two SCNT:parthenote traits.

Testing of correlations in expression between genes

The genetic data indicate cooperative interactions between multiple loci. Additionally, the gene expression data above indicate that more than one of the genes tested likely contribute to processes that specifically affect cloning outcome. We therefore tested for cooperativity between genes at the level of mRNA expression that could contribute to phenotype. This analysis focused on genes displaying individual expression correlations with phenotype. The primary significant LRS interval on chr 17 encompasses two genes (*Epb4.1l3* and *Dlgap1*) and nearby *Arhgap28*, all of which fulfill expectations of differential expression between B6 and D2 oocytes, haplotype effect, and expected associations between expression and developmental outcomes among BXD strains. Five other chr 17 genes (*Smchd1*, *Tgif1*, *Ndc80*, *Lclat1*, *Ypel5*) exerted lesser effects or effects only partially specific to SCNT embryos. For the chr 4 interval, the *Runx1t1* gene remains as the only candidate within the defined significance interval, and although it does not show a strong fit to the expected pattern, it displays an association with SCNT four-cell to blastocyst conversion independent of any parthenote effects, indicating that it likely contributes to overall outcome for cloned embryos. Four other chr 4 genes (*Car8*, *Asph*, *Chd7*, *Ccne2*) may also contribute to SCNT embryo development. For the chr 1 interval, the *Mfsd9* gene from near the significance interval appears most likely to contribute to outcome. Two other genes from chr 1 (*Phf3* and *D1Bwg0212e*) may contribute to clone development, whereas *Txndc9* and *Eif5b* may exert nonspecific effects. Thus, of the 26 genes tested on all 28 strains, 5 stand out as major candidates, and another 11 display an elevated likelihood of providing supportive contributions (Figure 2). To gain further insight, we tested for cooperativity among genes in terms of expression correlation with developmental outcomes (Table S8).

The *Epb4.1l3* mRNA displayed significant positive expression correlations with *Dlgap1*, *Mfsd9*, *Ypel5*, *Runx1t1*, *Chd7*, and *Esrp1* and significant negative correlations with *Arhgap28*, *Ndc80*, *Spast*, *Txndc9*, *Smchd1*, *Phf3*, and *Eif5b*. The *Dlgap1* mRNA displayed significant positive correlations in expression with *Epb4.1l3*, *Arhgap28*, *Mfsd9*, *Ndc80*, *Chd7*, *Esrp1*, *Car8*, and *Rab2a* and negative correlations for *Tmem182*, *Txndc9*, *Ccne2*, *Pdcl3*, *Tgif1*, and *Eif5b*. The *Arhgap28* gene showed significant positive expression correlations with *Dlgap1*, *Ndc80*, *Ypel5*, *Spast*, *Smchd1*, *Phf3*, and *Car8* and negative correlations with *Epb4.1l3*, *Ccne2*, *Pdcl3*, and *Lclat1*. Thus there are significant correlations between the expression patterns of all three of the primary chr 17

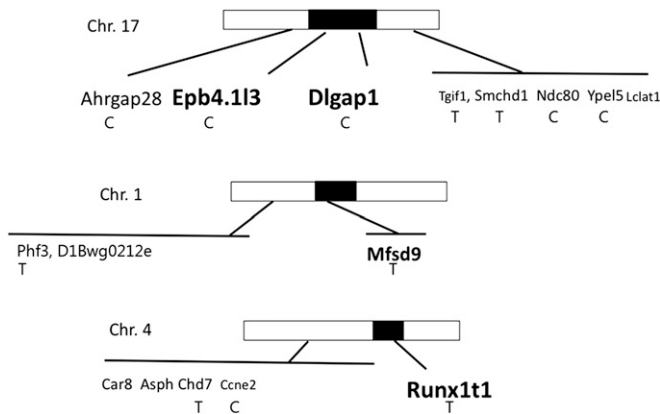


Figure 2 Summary of identified candidate genes. Genes having the most significant genetic and expression associations with phenotype are denoted by boldface type. Progressively smaller type sizes denote genes with progressively lesser associations but apparent SCNT-specific phenotype effects. C denotes cytoskeletal or spindle associated proteins. T denotes transcription and chromatin regulators.

genes with each other and with other genes. Correlations in expression between *Epb4.113*, *Runx1t1*, and *Mfsd9* are consistent with their effects on conversion from four-cell to blastocyst stage in the SNCT:parthenote data (Table 4) and provide a potential avenue for a cooperative interaction among the three significance intervals on chr 1, 4, and 17.

Ingenuity pathway analysis

To test further for cooperativity between the genes examined in this study, we undertook a biofunction and pathway analysis using the Ingenuity Pathway Analysis (IPA) program. One utility in the IPA program is a search of the IPA database for overrepresentation of members of a gene list among known biological functions and pathways. This analysis reveals known associations with two or more genes in a common biological function and indicates whether such functions are associated with a given experimental condition. Several potential gene associations were identified using the list of 26 genes displaying significant associations between expression and cloning traits (Table S9). One was the combination of *Dlgap1*, *Phf3*, *Rab2a*, and *Spast*, encompassing genes from chr 1, 4, and 17 regions. Another combination was *Aff3*, *Asph*, and *Chd7* from chromosomes 1 and 4. These combinations were retrieved for functions related to cell signaling and morphogenesis. There were many other combinations of just two genes. The *Epb4.113* gene occupied combinations with *Dlgap1*, *Asph*, *Spast*, and *Car8* and was connected indirectly to other genes via the other biofunction combinations.

A second utility offered by the IPA program is the ability to observe networks and pathways of interactions, both among members of the query gene list and with genes not on the list. Two networks were retrieved for the 26-gene query. One network contained 9 members of the list and another contained 15 members, indicating strong functional association among the 26 genes. Both networks have at their centers

ubiquitin C (UBC), indicating that many of the candidate genes tested are regulated directly or indirectly by protein ubiquitination. Additionally, Network 1 (Figure 3A) indicated significant connectivity for EPB4.113 and NDC80, as well as HNF4A and NFKB. Network 1 was modified by the inclusion of the ezrin–radixin–moesin complex, known to associate with EPB4.113 and with other actin-associated molecules such as TXNDC9 and TBC1D8, particularly in association with the plasma membrane where microfilaments and microtubules can provide crucial structure to facilitate signaling interactions. Network 2 (Figure 3B) included DLGAP1 as another key regulator of signaling at the plasma membrane. Note that the two networks can be connected via UBC. Each of the two networks contains one of the top chr 17 candidates from the region showing significant LRS values (*Epb4.113* and *Dlgap1*) connected to UBC and downstream to many potential mediators, including a range of nuclear factors that include *Runx1t1* from the chr 4 interval with a significant LRS value and *Tgif1* from near the chr 17 significance interval. Neither network incorporated *Mfsd9* or *Tmem182*, the two genes located adjacent to the chr 1 significance region, but other chr 1 genes (*Phf3*, *Txnac9*, *Aff3*, *Pdcl3*, and *Tbc1d8*) were present.

Because the genetic analysis indicated a possible interaction of the chr 17 interval with a region on chr 6, we also combined the 26 genes here with genes from the potential interacting region on chr 6 and submitted this combined list for IPA analysis. This yielded four networks, one of which included *Dlgap1* and one that included *Epb4.113* (Figure 3, C and D). In general, the chr 6 gene associations were via UBC and HNF4A as above (Figure 3C, Figure S1, and Figure S2). None of the four networks indicated direct dependent interactions between the chr 6 genes and any of the 26 genes tested. Array data indicated that the *Aak1*, *Antxr1*, *Gfpt1*, *Copg*, *Rab7*, *Sec61a1*, and *Pdzrn3* mRNAs are expressed in MII oocytes, with *Antxr1* (lower in D2) and *Pdzrn3* (higher in D2) displaying >25% differences in expression between B6 and D2, both of which reside in the network shown in Figure 2, which incorporates actin and clathrin as key components.

Gene sequence variations between haplotypes for candidate genes

Because sequence variation could affect protein activity and hence gene function apart from differences in mRNA expression abundance, we compared the B6 and D2 sequences for polymorphisms (Tables 5 and Table S10). Seventeen of the 26 genes studied in detail display polymorphisms in the 3'-UTR. Five of the genes studied (*Phf3*, *Pdcl3*, *Arhgap28*, *Ndc80*, and *Spast*) display polymorphisms affecting protein-coding region. Notable among these is the *Arhgap28* gene, which displays numerous polymorphisms in the 3'-UTR and two genetic variants in the coding region. This is the only gene among the 26 candidates and lying in or near the intervals with significant LRS values that displays variants in the coding region. The *Phf3*, *Pdcl3*, *Ndc80*, and *Spast* genes also display genetic variants in the coding regions. Polymorphisms in the 3'-UTRs for some mRNAs

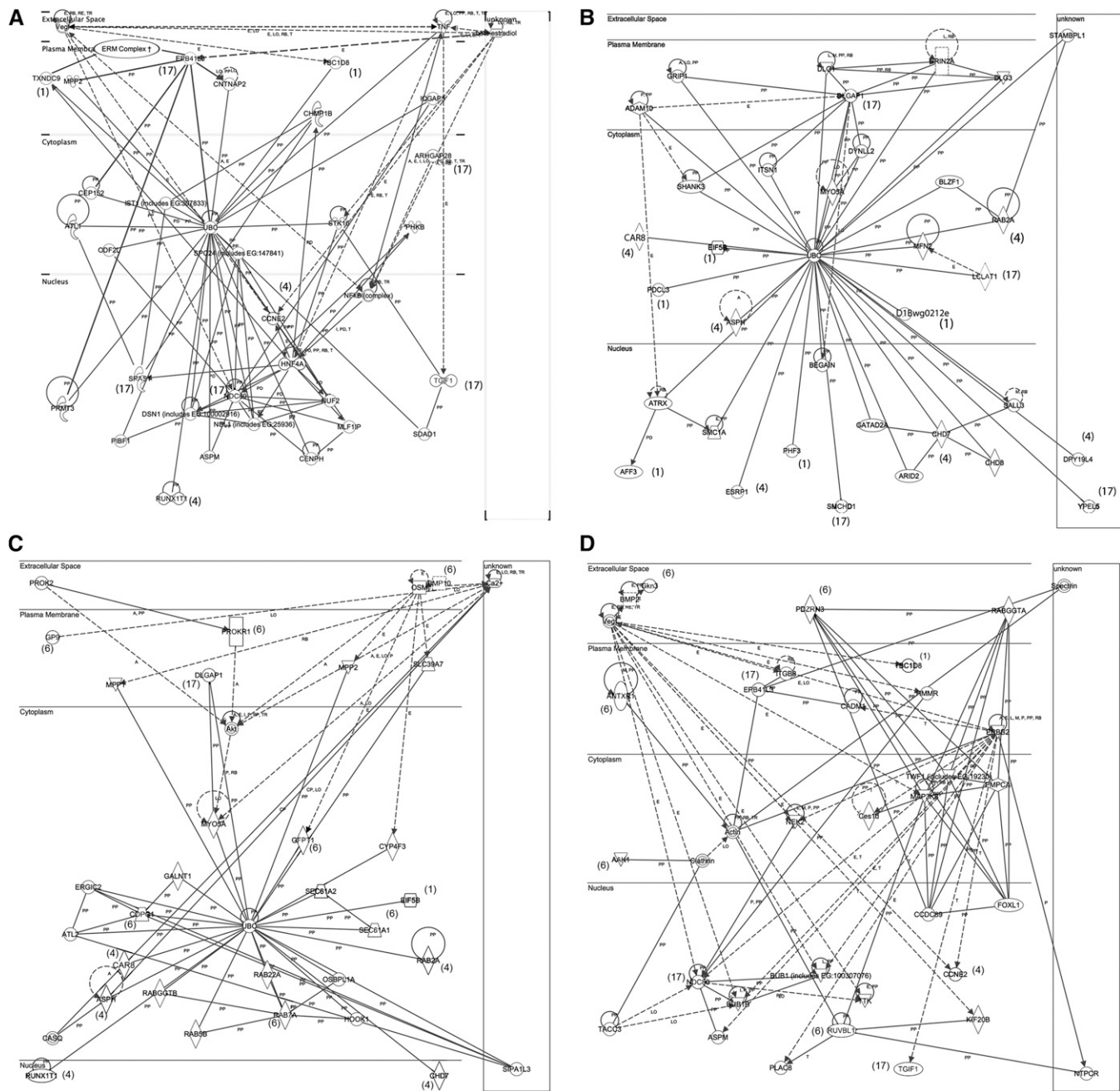


Figure 3 Ingenuity pathway analysis networks summarizing gene interactions among the 26 genes assayed for expression on all 28 strains (A and B) and these same 26 genes combined with genes from the potential interacting locus on chr 6 (C and D). Numbers in parentheses indicate chr assignments. PP, protein–protein interaction; PD, protein–DNA interaction; E, expression; A, activation; T, transcription; RB, regulation of binding; I, inhibition; LO, localization; CP, chemical–protein interaction; M, biochemical modification; solid line, binding only; line with arrow, downstream effect; broken line, indirect interaction; vertical diamond, enzyme; horizontal diamond, peptidase; horizontal oval, transcription factor; downward triangle, kinase; upward triangle, phosphatase; circle, other.

may also contribute to the observed differences in oocyte expression.

Discussion

For the first time, a systems genetics approach has been applied to the analysis of variation in oocyte composition associated with the ability of different genotypes of oocytes

to support early development of cloned embryos made by somatic cell nuclear transfer. The results provide new insight into clone biology, oocyte quality, and key early processes in mammalian embryogenesis. Overall, the analysis yielded polymorphic candidate genes related to two functional categories: (1) microtubule- and microfilament-associated proteins associated with the subcortical cytoskeletal network and spindle, and (2) a small number of proteins related to

Table 5 Summary of polymorphisms between B6 and D2 haplotypes for selected genes

Gene	Gene ID	Chr	No. variants	NS SNPs coding region	No. insertions or deletions coding region	No. SNPs 3'-UTR in variants from column 4	No. insertions or deletions 3'-UTR in variants from column 4
Genes in or near significance intervals							
Mfsd9	211798	1	1				
Tmem182	381339	1	1				
Runx1t1	12395	4	3				2, 2, 2
Arhgap28	268970	17	1	1	1	28	3
Epb4.1l3	13823	17	1				
Dlgap1	224997	17	4			0, 1, 1, 1	4, 1, 4, 1
Tgjf1	21815	17	5			2, 2, 2, 2, 2	
Other genes in suggestive intervals							
Phf3	213109	1	1	3	1	2	
Txndc9	98258	1	1			45	9
Eif5b	226982	1	1				
Aff3	16764	1	1				
Pdcl3	68833	1	1	1		1	
Tbc1d8	54610	1	1				
D1Bwg0212e	52846	1	1				
Car8	12319	4	1			65	9
Rab2a	59021	4	1			1	
Chd7	320790	4	1			1	1
Asph	65973	4	10			0, 4, 4, 5, 5, 5, 5, 5, 8	2, 0, 2, 1, 1, 1, 1, 0, 1, 1
Ccne2	12448	4	2				1, 1
Dpy19l4	381510	4	1				
Esrp1	207920	4	1				
Smchd1	74355	17	1			1	1
Ndc80	67052	17	1	1		2	
Ypel5	383295	17	1			6	2
Lclat1	225010	17	3			3, 3, 3	
Spast	50850	17	2	1, 1		9, 9	
Zfp161	22666	17	1				

transcriptional control and chromatin remodeling. The analysis revealed a major locus controlling cloning outcome on chr 17, with additional regions on chr 1 and 4 (Figure 3).

The strongest genetic and expression-phenotype associations were derived for two genes on chr 17 that encode cytoskeletal scaffolding proteins, *Epb4.1l3* and *Dlgap1*, yielding the novel discovery that cytoskeletal architecture plays a key and specific role in meeting specific developmental requirements of cloned embryos. Both *Dlgap1* and *Epb4.1l3* are components of the cortical cytoskeleton network and likely play roles in supporting cellular signaling. The *Epb4.1* family comprises scaffolding proteins that interact with the ezrin–radixin–moesin complex and play a role in tethering the cortical actin–spectrin complex to the plasma membrane, regulating cell shape, intercellular junctions, ion balance, signaling, and control of cellular proliferation (Kuns *et al.* 2005; Terada *et al.* 2005; Cifuentes-Diaz *et al.* 2011). *Dlgap1* encodes a scaffold protein also known as GKAP/SAPAP1, which controls receptor functioning as well as microtubule dynamics and organization near the cell cortex and promotes centrosome positioning (Manneville *et al.* 2010). Hence, these two proteins are positioned to exert profound effects on diverse cellular processes and are the strongest candidates for playing a role in cloned embryo development. *Arhgap28* encodes a signal transduction protein that may interact with the cor-

tical cytoskeletal complex. The *Epb4.1l3* gene was expressed more highly in D2 oocytes whereas the *Dlgap1* gene was expressed less in the D2 oocytes than in the B6 and B6D2 F1 oocytes. The *Epb4.1l3* gene expression was positively associated with SCNT embryo from two cell to four cell and blastocyst but its SCNT-specific component appears to be negative. The *Dlgap1* gene was expressed at a greatly reduced level in D2 oocytes and displayed a negative SCNT-specific effect and generally negative effects that were not limited to clones. These data are most consistent with a positive effect of the D2 haplotype in this region on cloned embryo development mediated by lower *Dlgap1* expression and non-SCNT-specific positive effects of *Epb4.1l3* at early cleavage stages.

The expression *Arhgap28* was also associated strongly with cloning phenotype, displaying a specific negative association with cloning outcome. Other candidate genes were related to cytoskeletal function as well. TXNDC9 (aka PHLIP3), a phosphatase, is required for proper actin and tubulin function (Stirling *et al.* 2006), and hence could interact directly or indirectly with *Epb4.1l3* and *Dlgap1* at the cortex. Interestingly, another gene studied on chr 1, *Pdcl3*, encodes another phosphatase that also promotes cytoskeletal remodeling (Hayes *et al.* 2011) and could likewise play a role in controlling the cortical cytoskeleton. EIF5B could positively affect protein translation (Lebaron *et al.* 2012). *Spast* encodes a microtubule-severing

protein (Fassier *et al.* 2012) and thereby contributes to cytoskeleton regulation. Three other expressed chr 17 genes from a suggestive interval but not included in our analysis due to uncertain functional relevance (*Memo1* and *Myl12a*, *Myl12b*) encode regulators of myosin contractility and cellular motility. The qRT-PCR results for one of these genes on B6, D2, and B6D2 F1 oocytes revealed only modest differences in mRNA expression.

This novel putative role for cytoskeletal proteins to meet the specific developmental needs of cloned embryos could reflect a specific need to restore cytoskeletal architecture after SCNT. This architecture may provide essential scaffolding functions that enable autocrine and paracrine signals to be transmitted inwardly to the nucleus, as well as enabling crucial homeostatic processes at the surface. *Asph* encodes a protein that post-translationally modifies epidermal growth factor domains in many proteins, deficiency for which is associated with later developmental defects (Dinchuk *et al.* 2002). The cytoskeletal architecture may also play crucial roles in controlling spindle formation and positioning or the positioning of organelles such as endoplasmic reticulum and mitochondria. ER positioning affects protein trafficking as well as calcium signaling (Soboloff *et al.* 2012). Mitochondrial positioning in close proximity to the genome could be important for providing ATP for reprogramming.

Another interesting possibility is that the cytoskeletal architecture plays a key role in establishing cellular potency. Other studies have pointed to essential roles played by a so-called subcortical maternal complex and cytoplasmic lattices, with potential roles in translational control and ultimately regulation of subsequent embryonic processes in mouse two-cell embryos (Li *et al.* 2008; Ohsugi *et al.* 2008; Yurttas *et al.* 2008; Kim *et al.* 2010; Kan *et al.* 2011). Even earlier studies reported interesting associations between microtubule acetylation, localization to the cortical region at the basal side of blastomeres, and subsequent partitioning to the inner cells, so that the microtubules might contribute to determining cell fate (Houliston and Maro 1989). It should prove interesting to discover whether the candidate gene products identified here, particularly EPB4.1L3 and DLGAP1, interact with subcortical maternal complex or other cytoskeletal elements to control early embryo development and whether this cytoskeletal architecture plays a regulative role in determining developmental potency and early cellular specializations.

It is also intriguing that some of the significant associations revealed here relate to spindle formation and function. There are significant protein composition deficits in the spindles that form in cloned constructs before activation and in mitotic spindles of at least the first couple of cell cycles (Miyara *et al.* 2006). Chromosome congression defects, mitotic errors, and aneuploidies in individual blastomeres of cloned embryos may be one consequence of this (Nolen *et al.* 2005; Miyara *et al.* 2006; Mizutani *et al.* 2012), reducing the number of viable cells and overall embryo viability. One major defect in these spindles is a deficiency in clathrin heavy chain, which bundles together microtubules and promotes spindle forma-

tion. Enhancement of clathrin heavy-chain expression improves chromosome congression in cloned embryos (Han *et al.* 2010b). The data here suggest that variations in expression of other proteins may compound these spindle defects, so that the rate of aneuploidies observed could vary with recipient oocyte genotype. One gene examined here, *Ndc80*, regulates oocyte spindle formation, chromosome alignment, and cell-cycle progression (Sun *et al.* 2011) and is associated with the kinetochore where it regulates microtubule dynamics (Umbreit *et al.* 2012). *Ccne2* is associated with *Ndc80* in the IPA analysis and could be associated with mediating checkpoint control. YPEL5 associates with the centrosome and spindle and promotes cell proliferation (Hosono *et al.* 2010). Proteins such as NDC80 and SPAST along with DLGAP1 may work together to regulate spindle or centrosome formation and function in cloned constructs. Further studies of how genetic variation in the expression of these proteins interacts with spindle deficiencies arising from the SCNT method should provide new insight into how the overall process of spindle formation is regulated. Moreover, understanding the roles played by these genes in oocyte spindle biology could provide new understanding related to the exponential increase in oocytes having defective spindles and chromosomal aneuploidies with age and onset of female reproductive senescence (Hunt and Hassold 2008) and may enable better management of this decline based on patient genotype information.

Although the major result from this analysis is a focus on cytoskeleton-associated proteins, this is not to discount the potential importance of transcription regulators such as *Runx1t1*, *Smchd1*, and *Chd7*. A significant role for these proteins is indicated by the identification of the intervals that contain these genes as having significant (*Runx1t1*) or suggestive (*Chd7*, *Smchd1*) LRS values. Stronger associations of *Chd7* and *Smchd1* might emerge with analysis of additional genotypes. Even lacking significant LRS values for these suggestive regions, the correlations between their expression and phenotypic traits among the BXD strains and the known biofunctions of these genes indicate that further study of these genes for roles in normal and cloned development is warranted.

Runx1t1 displayed a significant negative expression association with the SCNT and SCNT:parthenote four-cell to blastocyst transition traits. This indicates that the *Runx1t1* gene exerts a specific negative effect on overall cloned embryo development. *Runx1t1* appears in a gene network along with *Epb4.1l3* and *Arhgap28* (Figure 2A). RUNX1T1 (aka ETO) is a transcription factor that is joined to AML1 by chromosomal translocation to generate a leukemia gene, binds to DNA, and recruits histone deacetylase to repress gene expression (Erickson *et al.* 1994; Gelmetti *et al.* 1998). Increased RUNX1T1 activity could thus inhibit development.

The specific negative relationships seen between expression and clone development for *Chd7* and *Smchd1* may reflect effects on nuclear reprogramming or X chromosome regulation. CHD7 is a chromodomain helicase that either

negatively or positively modulates gene expression, including ES-cell-specific genes, although negative regulation is described as the more direct effect (Schnetz *et al.* 2010). CHD7 colocalizes in ES cells with POU5F1 (OCT4), SOX2, and NANOG and negatively modulates many genes selectively expressed in ES cells. SMCHD1 plays a key role in X-chromosome inactivation (Blewitt *et al.* 2008; Gendrel *et al.* 2012), which is also aberrant in cloned embryos (Nolen *et al.* 2005; Jiang *et al.* 2008; Inoue *et al.* 2010). It will be very interesting to determine the roles of these two factors in reprogramming during cloning and whether they might aid *in vitro* reprogramming by exogenous factors to make induced pluripotent stem cells.

Another transcription factor gene, *Zfp161*, lies within the chr 17 significance interval but was excluded on the basis of a lack of expression correlation with developmental phenotypes of the initial 6 BXD lines studied. This gene represses *Myc* (Sobek-Klocke *et al.* 1997). *Myc* promotes cell proliferation in stem cells and at later stages (Yamanaka 2008), but overexpression has little effect on early cleavage (Pan and Schultz 2011). While MYC may contribute to cell-cycle regulation and possible stress responses, particularly in advanced stage preimplantation embryos (Xie *et al.* 2007), the lack of a correlation between *Zfp161* expression and clone development argues against a specific role here. Additionally, the absence of genetic polymorphism in the coding region (Table 4 and Table S9) argues against a genetic effect at the level of protein structure.

We note the recent discovery that genome scanning approaches correlating genetic variants with phenotypic differences, such as that employed here, have the potential for yielding novel noncoding regulatory elements, such as enhancers and other chromatin regulatory elements (Dunham *et al.* 2012). The interactions of these elements can extend over large distances along the chromosome. We note, however, that the sizes of the combined significant and suggestive candidate intervals included in our study are large (12.7-cM chr 1, 7-cM chr 4, and 9.5-cM chr 17) and so provided the opportunity to detect significant variations in affected target genes. By evaluating the levels of expression and comparative expression levels between B6, D2, and B6D2 F1 genotypes for genes throughout these regions, we have provided a rigorous coverage of known gene products most likely to be affected by regulatory elements that could exist in the intervals with significant LRS values. Moreover, our identification of several genes that display strong and significant correlations between expression and phenotype, both individually and in combination, while also demonstrating known functional relationships in gene networks, provides high confidence in the newly ascribed relationships of these genes to clone biology.

Other genes examined in this study display relationships between expression and development and thus are likely to contribute to the overall success of cloned embryo development. Four genes displayed notable associations between expression and development that were not specific to

cloned embryos (*Txndc9*, *Eif5b*, *Tmem182*, *Spast*). The *Txndc9* and *Eif5b* genes are a bidirectionally coregulated gene pair (Garcia and Nagai 2011). These two genes displayed negative expression associations with development of both cloned and parthenogenetic embryos, so the associations were not specific to cloned embryos. Some of the associations seen were not in agreement for the two genes, raising some question about their relevance. However, it is noted that the zygotic REDOX state can affect postnatal phenotype (Banrezes *et al.* 2011). Participation of *Txndc9* in such regulation could contribute to SCNT development. Other genes displayed a combination of specific and non-specific associations between expression and development at different stages. Early, specific associations were seen for genes on chr 4 (*Ccne2*) and chr 17 (*Tgif1*, *Smchd1*, *Car8*, *Ypel5*, *Esrp1*, *Lclat1*). Later stage-specific associations were seen for genes on chr 1 (*D1Bwg0212e*), chr 4 (*Chd7*, *Car8*, *Asph*), and chr 17 (*Ndc80*).

Still other genes not selected for detailed study but lying within the candidate intervals could be proposed to play a role in cloned embryo development. DNA repair genes, for example, could be important for repairing DNA damage in the somatic donor nuclei, or damage that might arise during SCNT, and could also play roles in DNA replication. DNA base excision repair can contribute to epigenetic transitions (Sarkies *et al.* 2010; Seisenberger *et al.* 2013). Of the two DNA repair genes residing within the candidate intervals, *Rev1* displayed little difference in expression between B6, D2, and B6D2 F1 genotypes and was excluded on that basis, while *Rad54b* mRNA was expressed at a low level in MII oocytes and displayed a modest difference in expression between B6, D2, and B6D2 F1 oocytes on arrays. Noncoding RNAs present in the ooplasm could be proposed to play important roles. We examined noncoding RNA genes in or near the intervals with significant LRS values without positive results. As described above, these genes were typically excluded as candidates on the basis of two or more criteria including available expression data, making them far less likely candidates than those selected for analysis.

One final point to consider is what these results tell us about the determinants of oocyte quality and how this relates to clinical reproductive medicine outcomes. The differences in expression between MII oocytes of the different genotypes highlight the importance of not assuming that all oocytes are created equal. Indeed, there is substantial genetic variation in oocyte phenotype revealed among these BXD strains, which would be analogous to variation among family members; the amount of variation among a broader spectrum of individuals should be at least this great. This suggests that microsurgical approaches that assume uniformity among oocytes from different patients may reap unexpected outcomes. This also suggests that genetic data for patients could be useful in evaluating relative risks or likely success of clinical procedures and may be useful to modify clinical procedures to optimize them for specific individuals.

Acknowledgments

The authors are grateful to Robert W. Williams and Lu Lu, University of Tennessee Health Science Center, and Fernando Pardo-Manuel de Vilena for their guidance and encouragement in analyzing the data. We also thank Robert W. Williams and Susannah Varmuza for comments on the manuscript. This work was supported by a grant from the National Institutes of Health (NIH), National Institute of Child Health and Human Development, funded under the American Recovery and Reinvestment Act (ARRA), RC1HD063371, by the grant HD43092, and by the NIH Office of the Director, Comparative Medicine Branch, Office of Research Infrastructure Programs (ORIP) R24OD012221-12 to K.E.L.

Literature Cited

- Akagi, S., K. Matsukawa, E. Mizutani, K. Fukunari, M. Kaneda *et al.*, 2011 Treatment with a histone deacetylase inhibitor after nuclear transfer improves the preimplantation development of cloned bovine embryos. *J. Reprod. Dev.* 57: 120–126.
- Andreux, P. A., E. G. Williams, H. Koutnikova, R. H. Houtkooper, M. F. Champy *et al.*, 2012 Systems genetics of metabolism: the use of the bxd murine reference panel for multiscale integration of traits. *Cell* 150: 1287–1299.
- Banrezes, B., T. Sainte-Beuve, E. Canon, R. M. Schultz, J. Cancela *et al.*, 2011 Adult body weight is programmed by a redox-regulated and energy-dependent process during the pronuclear stage in mouse. *PLoS ONE* 6: e29388.
- Blewitt, M. E., A. V. Gendrel, Z. Pang, D. B. Sparrow, N. Whitelaw *et al.*, 2008 SmcHD1, containing a structural-maintenance-of-chromosomes hinge domain, has a critical role in X inactivation. *Nat. Genet.* 40: 663–669.
- Bothe, G. W., V. J. Bolivar, M. J. Vedder, and J. G. Geistfeld, 2004 Genetic and behavioral differences among five inbred mouse strains commonly used in the production of transgenic and knockout mice. *Genes Brain Behav.* 3: 149–157.
- Bryant, C. D., 2011 The blessings and curses of C57BL/6 substrains in mouse genetic studies. *Ann. N. Y. Acad. Sci.* 1245: 31–33.
- Bui, H. T., H. J. Seo, M. R. Park, J. Y. Park, N. V. Thuan *et al.*, 2011 Histone deacetylase inhibition improves activation of ribosomal RNA genes and embryonic nucleolar reprogramming in cloned mouse embryos. *Biol. Reprod.* 85: 1048–1056.
- Campbell, K. H., J. McWhir, W. A. Ritchie, and I. Wilmut, 1996 Sheep cloned by nuclear transfer from a cultured cell line. *Nature* 380: 64–66.
- Chavatte-Palmer, P., S. Camous, H. Jammes, N. Le Cleac'h, M. Guillomot *et al.*, 2012 Review: placental perturbations induce the developmental abnormalities often observed in bovine somatic cell nuclear transfer. *Placenta* 33(Suppl): S99–S104.
- Chen, L., D. Wang, Z. Wu, L. Ma, and G. Q. Daley, 2010 Molecular basis of the first cell fate determination in mouse embryogenesis. *Cell Res.* 20: 982–993.
- Chung, Y. G., M. R. Mann, M. S. Bartolomei, and K. E. Latham, 2002 Nuclear-cytoplasmic “tug of war” during cloning: effects of somatic cell nuclei on culture medium preferences of preimplantation cloned mouse embryos. *Biol. Reprod.* 66: 1178–1184.
- Chung, Y. G., S. Ratnam, J. R. Chaillet, and K. E. Latham, 2003 Abnormal regulation of DNA methyltransferase expression in cloned mouse embryos. *Biol. Reprod.* 69: 146–153.
- Chung, Y. G., S. Gao, and K. E. Latham, 2006 Optimization of procedures for cloning by somatic cell nuclear transfer in mice. *Methods Mol. Biol.* 348: 111–124.
- Cifuentes-Diaz, C., F. Chareyre, M. Garcia, J. Devaux, M. Carnaud *et al.*, 2011 Protein 4.1B contributes to the organization of peripheral myelinated axons. *PLoS ONE* 6: e25043.
- Dinchuk, J. E., R. J. Focht, J. A. Kelley, N. L. Henderson, N. I. Zolotarjova *et al.*, 2002 Absence of post-translational aspartyl beta-hydroxylation of epidermal growth factor domains in mice leads to developmental defects and an increased incidence of intestinal neoplasia. *J. Biol. Chem.* 277: 12970–12977.
- Dunham, I., A. Kundaje, S. F. Aldred, P. J. Collins, C. A. Davis *et al.*, 2012 An integrated encyclopedia of DNA elements in the human genome. *Nature* 489: 57–74.
- Eggan, K., H. Akutsu, K. Hochedlinger, W. Rideout 3rd, R. Yanagimachi *et al.*, 2000 X-chromosome inactivation in cloned mouse embryos. *Science* 290: 1578–1581.
- Erickson, P. F., M. Robinson, G. Owens, and H. A. Drabkin, 1994 The ETO portion of acute myeloid leukemia t(8;21) fusion transcript encodes a highly evolutionarily conserved, putative transcription factor. *Cancer Res.* 54: 1782–1786.
- Fassier, C., A. Tarrade, L. Peris, S. Courageot, P. Mailly *et al.*, 2012 Microtubule-targeting drugs rescue axonal swellings in cortical neurons from spastin knock-out mice. *Dis. Model Mech.* 6: 72–83.
- Gao, S., and K. E. Latham, 2004 Maternal and environmental factors in early cloned embryo development. *Cytogenet. Genome Res.* 105: 279–284.
- Gao, S., Y. G. Chung, J. W. Williams, J. Riley, K. Moley *et al.*, 2003 Somatic cell-like features of cloned mouse embryos prepared with cultured myoblast nuclei. *Biol. Reprod.* 69: 48–56.
- Gao, S., E. Czirr, Y. G. Chung, Z. Han, and K. E. Latham, 2004 Genetic variation in oocyte phenotype revealed through parthenogenesis and cloning: correlation with differences in pronuclear epigenetic modification. *Biol. Reprod.* 70: 1162–1170.
- Garcia, S. A., and M. A. Nagai, 2011 Transcriptional regulation of bidirectional gene pairs by 17-beta-estradiol in MCF-7 breast cancer cells. *Braz. J. Med. Biol. Res.* 44: 112–122.
- Gelmetti, V., J. Zhang, M. Fanelli, S. Minucci, P. G. Pelicci *et al.*, 1998 Aberrant recruitment of the nuclear receptor corepressor-histone deacetylase complex by the acute myeloid leukemia fusion partner ETO. *Mol. Cell. Biol.* 18: 7185–7191.
- Gendrel, A. V., A. Apedaile, H. Coker, A. Termanis, I. Zvetkova *et al.*, 2012 SmcHD1-dependent and -independent pathways determine developmental dynamics of CpG island methylation on the inactive X chromosome. *Dev. Cell* 23: 265–279.
- Guillomot, M., G. Taghouti, F. Constant, S. Degrelle, I. Hue *et al.*, 2010 Abnormal expression of the imprinted gene Phlda2 in cloned bovine placenta. *Placenta* 31: 482–490.
- Hamatani, T., M. Ko, M. Yamada, N. Kuji, Y. Mizusawa *et al.*, 2006 Global gene expression profiling of preimplantation embryos. *Hum. Cell* 19: 98–117.
- Han, Z., R. Vassena, M. M. Chi, S. Potireddy, M. Sutovsky *et al.*, 2008 Role of glucose in cloned mouse embryo development. *Am. J. Physiol. Endocrinol. Metab.* 295: E798–E809.
- Han, Z., Y. Cheng, C. G. Liang, and K. E. Latham, 2010a Nuclear transfer in mouse oocytes and embryos. *Methods Enzymol.* 476: 171–184.
- Han, Z., C. G. Liang, Y. Cheng, X. Duan, Z. Zhong *et al.*, 2010b Oocyte spindle proteomics analysis leading to rescue of chromosome congression defects in cloned embryos. *J. Proteome Res.* 9: 6025–6032.
- Hayes, N. V., L. Josse, C. M. Smales, and M. J. Carden, 2011 Modulation of phosphoinositide-dependent protein kinase 3 (PDK3) levels promotes cytoskeletal remodeling in a MAPK and RhoA-dependent manner. *PLoS ONE* 6: e28271.
- Hosono, K., S. Noda, A. Shimizu, N. Nakanishi, M. Ohtsubo *et al.*, 2010 YPEL5 protein of the YPEL gene family is involved in the cell cycle progression by interacting with two distinct proteins RanBPM and RanBP10. *Genomics* 96: 102–111.

- Houlston, E., and B. Maro, 1989 Posttranslational modification of distinct microtubule subpopulations during cell polarization and differentiation in the mouse preimplantation embryo. *J. Cell Biol.* 108: 543–551.
- Humpherys, D., K. Eggan, H. Akutsu, A. Friedman, K. Hochedlinger *et al.*, 2002 Abnormal gene expression in cloned mice derived from embryonic stem cell and cumulus cell nuclei. *Proc. Natl. Acad. Sci. USA* 99: 12889–12894.
- Hunt, P. A., and T. J. Hassold, 2008 Human female meiosis: What makes a good egg go bad? *Trends Genet.* 24: 86–93.
- Inoue, K., T. Kohda, M. Sugimoto, T. Sado, N. Ogonuki *et al.*, 2010 Impeding Xist expression from the active X chromosome improves mouse somatic cell nuclear transfer. *Science* 330: 496–499.
- Jafari, S., M. S. Hosseini, M. Hajian, M. Forouzanfar, F. Jafarpour *et al.*, 2011 Improved in vitro development of cloned bovine embryos using S-adenosylhomocysteine, a non-toxic epigenetic modifying reagent. *Mol. Reprod. Dev.* 78: 576–584.
- Jiang, L., L. Lai, M. Samuel, R. S. Prather, X. Yang *et al.*, 2008 Expression of X-linked genes in deceased neonates and surviving cloned female piglets. *Mol. Reprod. Dev.* 75: 265–273.
- Kan, R., P. Yurttas, B. Kim, M. Jin, L. Wo *et al.*, 2011 Regulation of mouse oocyte microtubule and organelle dynamics by PADI6 and the cytoplasmic lattices. *Dev. Biol.* 350: 311–322.
- Kim, B., R. Kan, L. Anguish, L. M. Nelson, and S. A. Coonrod, 2010 Potential role for MATER in cytoplasmic lattice formation in murine oocytes. *PLoS ONE* 5: e12587.
- Kim, Y. J., K. S. Ahn, M. Kim, and H. Shim, 2011 Comparison of potency between histone deacetylase inhibitors trichostatin A and valproic acid on enhancing in vitro development of porcine somatic cell nuclear transfer embryos. *In Vitro Cell. Dev. Biol. Anim.* 47: 283–289.
- Kuns, R., J. L. Kissil, I. F. Newsham, T. Jacks, D. H. Gutmann *et al.*, 2005 Protein 4.1B expression is induced in mammary epithelial cells during pregnancy and regulates their proliferation. *Oncogene* 24: 6502–6515.
- Latham, K. E., 2004 Cloning: questions answered and unsolved. *Differentiation* 72: 11–22.
- Latham, K. E., 2005 Early and delayed aspects of nuclear reprogramming during cloning. *Biol. Cell* 97: 119–132.
- Latham, K. E., and R. M. Schultz, 2001 Embryonic genome activation. *Front. Biosci.* 6: D748–D759.
- Latham, K. E., J. I. Garrels, C. Chang, and D. Solter, 1992 Analysis of embryonic mouse development: construction of a high-resolution, two-dimensional gel protein database. *Appl. Theor. Electrophor.* 2: 163–170.
- Latham, K. E., S. Gao, and Z. Han, 2007 Somatic cell nuclei in cloning: strangers traveling in a foreign land. *Adv. Exp. Med. Biol.* 591: 14–29.
- Lebaron, S., C. Schneider, R. W. van Nues, A. Swiatkowska, D. Walsh *et al.*, 2012 Proofreading of pre-40S ribosome maturation by a translation initiation factor and 60S subunits. *Nat. Struct. Mol. Biol.* 19: 744–753.
- Lee, Y. S., K. E. Latham, and C. A. Vandevoort, 2008 Effects of in vitro maturation on gene expression in rhesus monkey oocytes. *Physiol. Genomics* 35: 145–158.
- Li, L., B. Baibakov, and J. Dean, 2008 A subcortical maternal complex essential for preimplantation mouse embryogenesis. *Dev. Cell* 15: 416–425.
- Livak, K. J., and T. D. Schmittgen, 2001 Analysis of relative gene expression data using real-time quantitative PCR and the 2^{-ΔΔC_T} (T). *Method. Methods* 25: 402–408.
- Mann, M. R., Y. G. Chung, L. D. Nolen, R. I. Verona, K. E. Latham *et al.*, 2003 Disruption of imprinted gene methylation and expression in cloned preimplantation stage mouse embryos. *Biol. Reprod.* 69: 902–914.
- Manneville, J. B., M. Jehanno, and S. Etienne-Manneville, 2010 Dlg1 binds GKAP to control dynein association with microtubules, centrosome positioning, and cell polarity. *J. Cell Biol.* 191: 585–598.
- Matoba, S., K. Inoue, T. Kohda, M. Sugimoto, E. Mizutani *et al.*, 2011 RNAi-mediated knockdown of Xist can rescue the impaired postimplantation development of cloned mouse embryos. *Proc. Natl. Acad. Sci. USA* 108: 20621–20626.
- Mekada, K., K. Abe, A. Murakami, S. Nakamura, H. Nakata *et al.*, 2009 Genetic differences among C57BL/6 substrains. *Exp. Anim.* 58: 141–149.
- Miyara, F., Z. Han, S. Gao, R. Vassena, and K. E. Latham, 2006 Non-equivalence of embryonic and somatic cell nuclei affecting spindle composition in clones. *Dev. Biol.* 289: 206–217.
- Mizutani, E., K. Yamagata, T. Ono, S. Akagi, M. Geshi *et al.*, 2012 Abnormal chromosome segregation at early cleavage is a major cause of the full-term developmental failure of mouse clones. *Dev. Biol.* 364: 56–65.
- Mtango, N. R., S. Potireddy, and K. E. Latham, 2008 Oocyte quality and maternal control of development. *Int. Rev. Cell. Mol. Biol.* 268: 223–290.
- Mtango, N. R., C. A. VandeVoort, and K. E. Latham, 2011 Ontological aspects of pluripotency and stemness gene expression pattern in the rhesus monkey. *Gene Expr. Patterns* 11: 285–298.
- Nolen, L. D., S. Gao, Z. Han, M. R. Mann, Y. Gie Chung *et al.*, 2005 X chromosome reactivation and regulation in cloned embryos. *Dev. Biol.* 279: 525–540.
- Ogura, A., K. Inoue, N. Ogonuki, J. Lee, T. Kohda *et al.*, 2002 Phenotypic effects of somatic cell cloning in the mouse. *Cloning Stem Cells* 4: 397–405.
- Ohgane, J., T. Wakayama, Y. Kogo, S. Senda, N. Hattori *et al.*, 2001 DNA methylation variation in cloned mice. *Genesis* 30: 45–50.
- Ohsugi, M., P. Zheng, B. Baibakov, L. Li, and J. Dean, 2008 Maternally derived FILIA-MATER complex localizes asymmetrically in cleavage-stage mouse embryos. *Development* 135: 259–269.
- Ozil, J. P., B. Banrezes, S. Toth, H. Pan, and R. M. Schultz, 2006 Ca²⁺ + oscillatory pattern in fertilized mouse eggs affects gene expression and development to term. *Dev. Biol.* 300: 534–544.
- Pan, H., and R. M. Schultz, 2011 Sox2 modulates reprogramming of gene expression in two-cell mouse embryos. *Biol. Reprod.* 85: 409–416.
- Pan, H., M. J. O'Brien, K. Wigglesworth, J. J. Eppig, and R. M. Schultz, 2005 Transcript profiling during mouse oocyte development and the effect of gonadotropin priming and development in vitro. *Dev. Biol.* 286: 493–506.
- Sarkies, P., C. Reams, L. J. Simpson, and J. E. Sale, 2010 Epigenetic instability due to defective replication of structured DNA. *Mol. Cell* 40: 703–713.
- Schnet, M. P., L. Handoko, B. Akhtar-Zaidi, C. F. Bartels, C. F. Pereira *et al.*, 2010 CHD7 targets active gene enhancer elements to modulate ES cell-specific gene expression. *PLoS Genet.* 6: e1001023.
- Seisenberger, S., J. R. Peat, T. A. Hore, F. Santos, W. Dean *et al.*, 2013 Reprogramming DNA methylation in the mammalian life cycle: building and breaking epigenetic barriers. *Philos. Trans. R. Soc. Lond. B Biol. Sci.* 368: 20110330.
- Sobek-Klocke, I., C. Disque-Kochem, M. Ronsiek, R. Klocke, H. Jockusch *et al.*, 1997 The human gene ZFP161 on 18p11.21-pter encodes a putative c-myc repressor and is homologous to murine Zfp161 (Chr 17) and Zfp161-rs1 (X Chr). *Genomics* 43: 156–164.
- Soboloff, J., B. S. Rothberg, M. Madesh, and D. L. Gill, 2012 STIM proteins: dynamic calcium signal transducers. *Nat. Rev. Mol. Cell Biol.* 13: 549–565.

- Stirling, P. C., J. Cuellar, G. A. Alfaro, F. El Khadali, C. T. Beh *et al.*, 2006 PhLP3 modulates CCT-mediated actin and tubulin folding via ternary complexes with substrates. *J. Biol. Chem.* 281: 7012–7021.
- Sun, S. C., D. X. Zhang, S. E. Lee, Y. N. Xu, and N. H. Kim, 2011 Ndc80 regulates meiotic spindle organization, chromosome alignment, and cell cycle progression in mouse oocytes. *Microsc. Microanal.* 17: 431–439.
- Svoboda, P., 2010 Why mouse oocytes and early embryos ignore miRNAs? *RNA Biol.* 7: 559–563.
- Taylor, B. A., 1972 Genetic relationships between inbred strains of mice. *J. Hered.* 63: 83–86.
- Terada, N., N. Ohno, H. Yamakawa, O. Ohara, and S. Ohno, 2005 Topographical significance of membrane skeletal component protein 4.1 B in mammalian organs. *Anat. Sci. Int.* 80: 61–70.
- Terashita, Y., S. Wakayama, K. Yamagata, C. Li, E. Sato *et al.*, 2012 Latrunculin a can improve the birth rate of cloned mice and simplify the nuclear transfer protocol by gently inhibiting actin polymerization. *Biol. Reprod.* 86: 180.
- Umbreit, N. T., D. R. Gestaut, J. F. Tien, B. S. Vollmar, T. Gonen *et al.*, 2012 The Ndc80 kinetochore complex directly modulates microtubule dynamics. *Proc. Natl. Acad. Sci. USA* 109: 16113–16118.
- Vassena, R., Z. Han, S. Gao, D. A. Baldwin, R. M. Schultz *et al.*, 2007a Tough beginnings: alterations in the transcriptome of cloned embryos during the first two cell cycles. *Dev. Biol.* 304: 75–89.
- Vassena, R., Z. Han, S. Gao, and K. E. Latham, 2007b Deficiency in recapitulation of stage-specific embryonic gene transcription in two-cell stage cloned mouse embryos. *Mol. Reprod. Dev.* 74: 1548–1556.
- Wagschal, A., and R. Feil, 2006 Genomic imprinting in the placenta. *Cytogenet. Genome Res.* 113: 90–98.
- Wang, L. J., H. Zhang, Y. S. Wang, W. B. Xu, X. R. Xiong *et al.*, 2011 Scriptaid improves in vitro development and nuclear reprogramming of somatic cell nuclear transfer bovine embryos. *Cell Reprogram* 13: 431–439.
- Wang, S., Z. Kou, Z. Jing, Y. Zhang, X. Guo *et al.*, 2010a Proteome of mouse oocytes at different developmental stages. *Proc. Natl. Acad. Sci. USA* 107: 17639–17644.
- Wang, X., R. Agarwala, J. A. Capra, Z. Chen, D. M. Church *et al.*, 2010b High-throughput sequencing of the DBA/2J mouse genome. *BMC Bioinformatics* 11(Suppl. 4): 1–2.
- Whitworth, K. M., J. Zhao, L. D. Spate, R. Li, and R. S. Prather, 2011 Scriptaid corrects gene expression of a few aberrantly reprogrammed transcripts in nuclear transfer pig blastocyst stage embryos. *Cell Reprogram* 13: 191–204.
- Xie, Y., W. Zhong, Y. Wang, A. Trostinskaia, F. Wang *et al.*, 2007 Using hyperosmolar stress to measure biologic and stress-activated protein kinase responses in preimplantation embryos. *Mol. Hum. Reprod.* 13: 473–481.
- Yamanaka, S., 2008 Induction of pluripotent stem cells from mouse fibroblasts by four transcription factors. *Cell Prolif.* 41 (Suppl. 1): 51–56.
- Yurttas, P., A. M. Vitale, R. J. Fitzhenry, L. Cohen-Gould, W. Wu *et al.*, 2008 Role for PADI6 and the cytoplasmic lattices in ribosomal storage in oocytes and translational control in the early mouse embryo. *Development* 135: 2627–2636.
- Zurita, E., M. Chagoyen, M. Cantero, R. Alonso, A. Gonzalez-Neira *et al.*, 2011 Genetic polymorphisms among C57BL/6 mouse inbred strains. *Transgenic Res.* 20: 481–489.

Communicating editor: J. C. Schimenti

GENETICS

Supporting Information

<http://www.genetics.org/lookup/suppl/doi:10.1534/genetics.112.148866/-/DC1>

Systems Genetics Implicates Cytoskeletal Genes in Oocyte Control of Cloned Embryo Quality

**Yong Cheng, John Gaughan, Uros Midic, Zhiming Han, Cheng-Guang Liang, Bela G. Patel,
and Keith E. Latham**

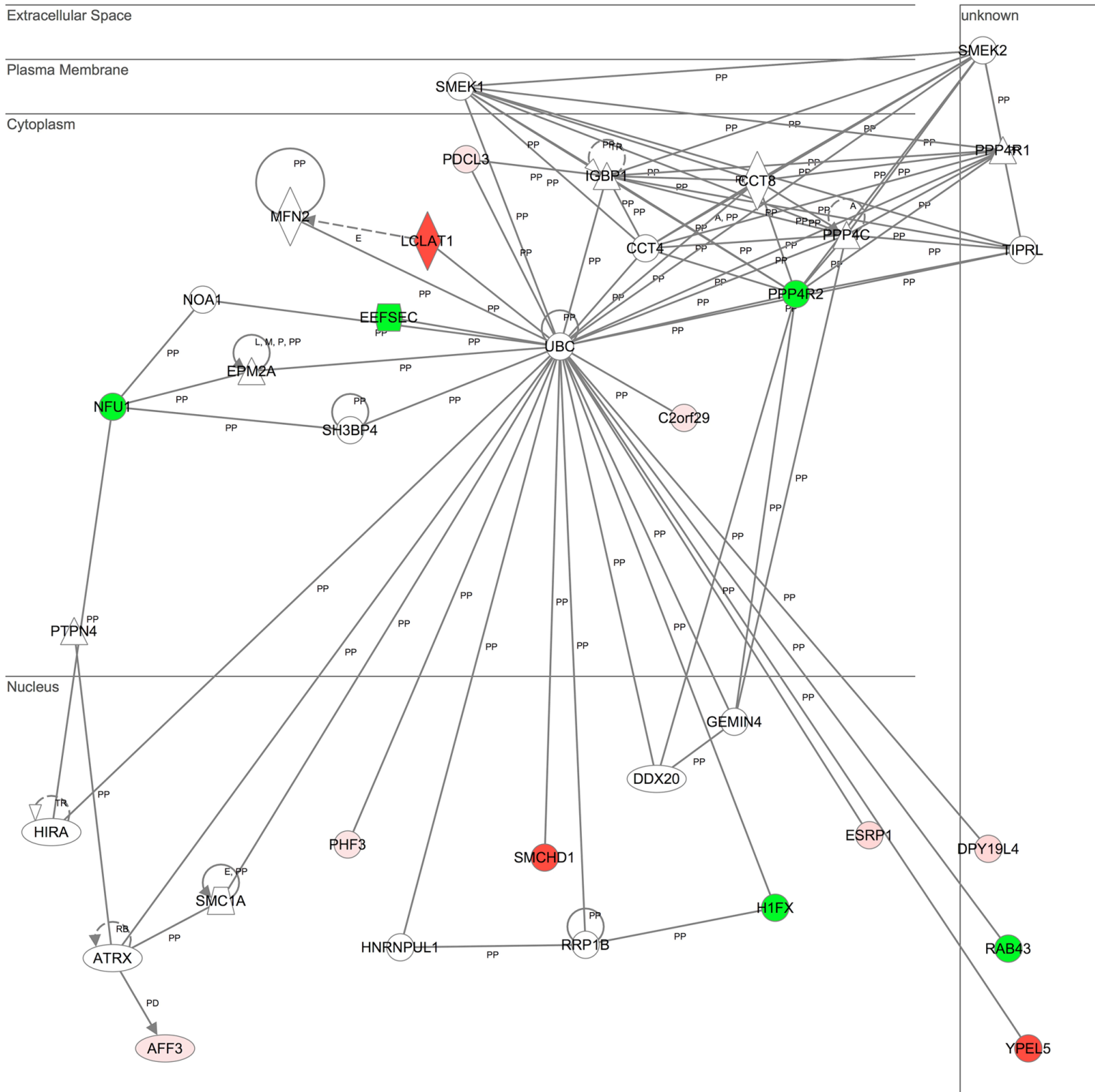


Figure S1 Ingenuity Pathway Analysis networks summarizing additional gene interactions amongst the 26 genes assayed for expression on all 28 strains combined with genes from the potential interacting locus on Chr 6. This network illustrates pathways with connections to UBC. Genes indicated in light, medium and dark shades of red correspond to genes from intervals on Chr 1, 4, and 17, respectively. Genes in green are from Chr 6. Numbers in parentheses indicate Chr assignments. PP,

protein-protein interaction; PD, protein-DNA interaction; E, expression; A, activation; T, transcription; RB, regulation of binding; I, inhibition; LO, localization; CP, chemical-protein interaction; M, biochemical modification; solid line, binding only; line with arrow, downstream effect; broken line, indirect interaction; vertical diamond, enzyme; horizontal diamond, peptidase; horizontal oval, transcription factor; down-pointing triangle, kinase; up-pointing triangle, phosphatase; circle, other.

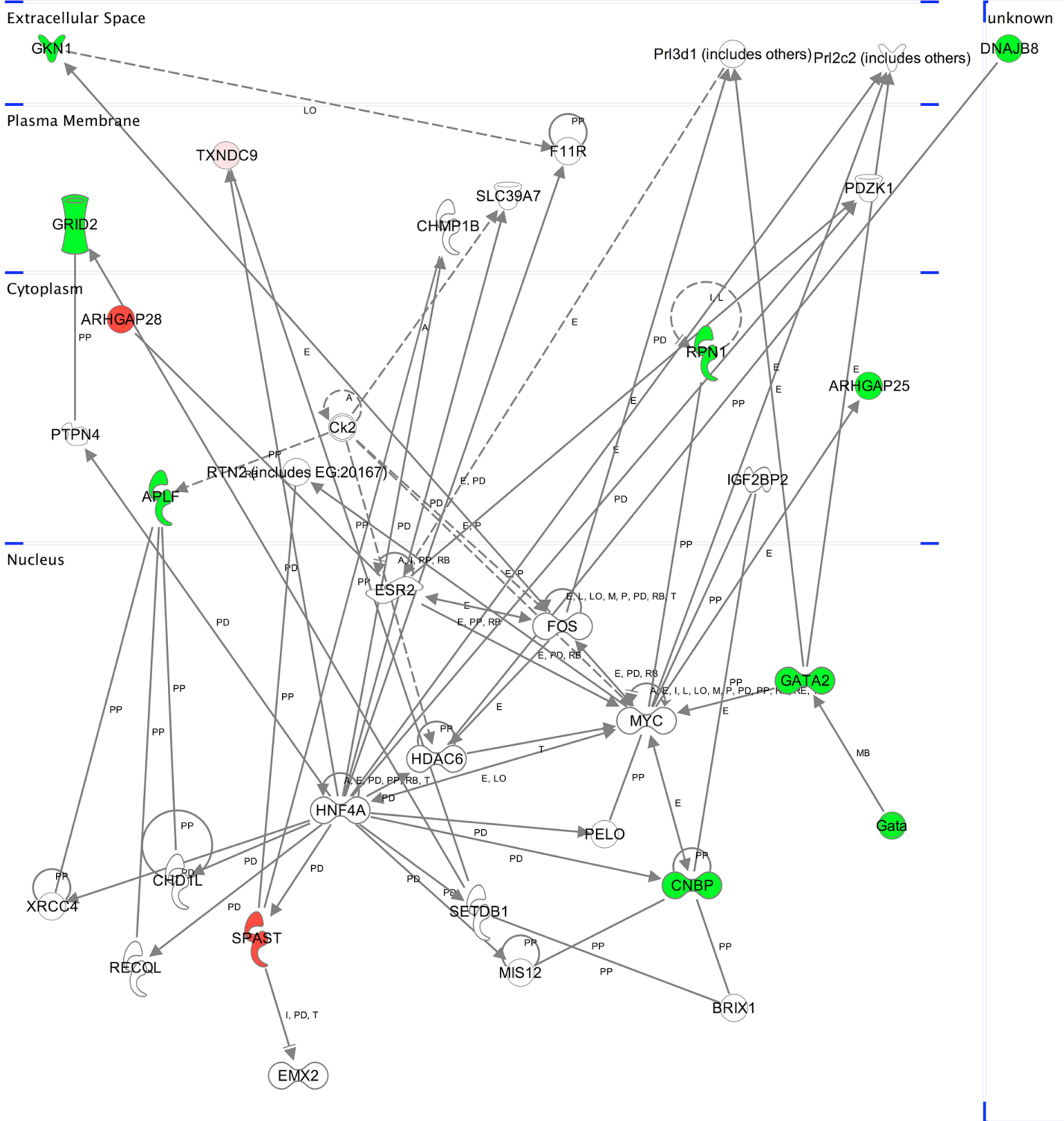


Figure S2 Ingenuity Pathway Analysis networks summarizing additional gene interactions amongst the 26 genes assayed for expression on all 28 strains combined with genes from the potential interacting locus on Chr 6. This network illustrates pathways with connections to HNF4A. Annotations and symbols are as described in Fig. S1.

Table S1. Primers used for qRT-PCR assay using the ABI System

Gene symbol	Assay ID
Chr 1	
Phf3	Mm01236622_m1
Txndc9	Mm00780643_s1
Eif5b	Mm01227247_m1
Rev1	Mm00450983_m1
Aff3	Mm01233112_m1
Pdcl3	Custom: For: GAAAGCAACTCAGCTGAAGAACAAA; Rev: CGCCGGCTTTCGTAATTCT; Rep:TCTCAGGAAAGACTATGTTC
Npas2	Mm00500848_m1
Tbc1d8	Mm00450644_m1
D1Bwg0212e	Mm00546872_m1
Rnf149	Mm01234645_m1
Mfsd9	Mm01237156_m1
Tmem182	Mm01239470_m1
Chr 4	
Tox	Mm00455231_m1
Car8	Mm00801469_m1
Rab2a	Mm00445482_m1
Chd7	Mm01219527_m1
Asph	Mm01211467_m1
Trp53inp1	Mm00458142_g1
Ccne2	Mm00438077_m1
Ints8	Mm00724177_m1
Dpy19l4	Mm01217524_m1
Esrp1	Mm01220929_m1
1110037F02Rik	Mm01217416_m1
Cdh17	Mm00490692_m1
Runx1t1	Mm00486771_m1
Chr 17	
Arhgap28	Mm00556965_m1
Epb4.1l3	Mm00469242_m1
Zfp161	Mm01236216_m1
Dlgap1	Mm00510688_m1
Tgif1	Mm01227699_m1
Lpin2	Mm00522390_m1
Smchd1	Mm00512253_m1
Ndc80	Mm00659108_m1
Clip4	Mm04209299_m1
Ypel5	Mm01233098_m1
Lclat1	Mm01237235_m1
Xdh	Mm00442121_m1
Dpy30	Mm01232913_g1
Spast	Mm01239546_m1
Yipf4	Mm00471331_m1
Birc6	Mm00464380_m1

Table S2. Marker regression analysis and interval mapping for parthenote development.

With Parents				
Blastocyst / 2 Cell				
Chrm.	Mb	Mb	Haplotype Incr. Trait	LRS
9	72.030418	72.952358	B6	10.34
	Suggestive LRS			10.33
	Significant			17.65
	Highly Significant			22.08
Blastocyst / 4 Cell				
Chrm.	Mb	Mb	Haplotype Incr. Trait	LRS
9	72.030418	72.952358	B6	11.172
13	120.05903	120.203852	B6	11.076
	Suggestive LRS			10.48
	Significant			18.39
	Highly Significant			23.06

Data for parthenote development (Table 1) were analyzed. Developmental transitions are as described in Table 1. LRS values for suggestive, significant and highly significant results are given for each trait.

Table S3. Marker regression analysis and interval mapping for clone:parthenote developmental ratio.

With Parents					Without Parents				
2 Cell / Constructs					4 Cell / 2 Cell				
Chr.	Mb	Mb	Haplotype Incr. Trait	LRS	Chr.	Mb	Mb	Haplotype Incr. Trait	LRS
16	69.289857		D2	9.35	8	31.744604	38.645978	D2	6.53
16	89.533119	89.590533	D2	9.428	Suggestive LRS				6.52
16	89.885517	90.609836	D2	10.255	Significant				9.89
Suggestive LRS				9.29	Highly Significant				12.02
Significant				14.92	Blastocyst / 4 Cell				
Highly Significant				17.95	Chr.	Mb	Mb	Haplotype Incr. Trait	LRS
4 Cell / 2 Cell					6	63.773076	64.613339	D2	8.779
Chr.	Mb	Mb	Haplotype Incr. Trait	LRS	Suggestive LRS				8.27
8	31.744604	38.645978	D2	6.81	Significant				13.45
8	39.28324	40.927342	D2	6.597	Highly Significant				16.65
16	45.072728	45.541112	D2	6.365					
Suggestive LRS				6.31					
Significant				9.52					
Highly Significant				10.99					
Blastocyst / 2 Cell									
Chr.	Mb	Mb	Haplotype Incr. Trait	LRS					
13	81.246253	83.876592	B6	8.217					
13	84.841126	91.275494	B6	8.517					
13	96.226476	96.283661	B6	8.383					
Suggestive LRS				7.85					
Significant				12.44					
Highly Significant				14.65					

Data for the ratio of SCNT:parthenote development (Table 1) were analyzed. Developmental transitions are as described in Table 1. LRS values for suggestive, significant and highly significant results are given for each trait.

Table S4. Composite analysis of loci interacting with markers in regions with significant LRS values for SCNT development.

Trait	Chr.	Significance Region Map Position (Mb)	Strain incr. trait	Composite Analysis (a) suggestive (b) significant interaction
4C:2C without parents	4	13.03102-13.76499	D	none
		rs13477566		
		gnf04.010.430		
	17	69.149197-71.101564	D	none
		rs13483086		
		rs3690010		
rs3701107				
BL:2C with parents	1	40-99094-42.21652	B	(suggestive) chr. 7 47.075-63.000; (suggestive) chr. 11 32.348-33.793; (suggestive) chr 11 35.534
		rs13475827		
		gnf01.037.906		
		gnf01.038.101		
		rs3671534		
		mCV23641317		
BL:2C without parents	17	69.149197-71.101564	D	(suggestive) chr. 6 86.953-88.668; (suggestive) chr. 6 100.818-101.44
		rs13483086		
		rs3690010		
		rs3701107		
		rs6176494		
		rs6176494		

The markers from each region used for the test are given, and genomic regions that may interact in determining the SCNT developmental progression (trait) specified are shown in rightmost column.

Table S5. Characteristics of genes in candidate intervals

Candidate Gene	Chromosome position in Build 37.2		Chromosome position in Build 38		Symbols (from build 38)	Detected in GV Proteome*	Detected in MII Proteome*	MAX GV Array Signal	MAX MII Array Signal	MAX Fold Change Array	MAX Fold change between B6,D2, B6D2F1 strains by qRT-PCR	MIN CT value amongst B6, D2, B6D2 F1 strains	SNPs in probeset with max signal (no. probes)	SNPs upstream of 5'UTR	SNPs in coding region	Functional Priority Group	Compartment	Biofunction/Location	
	start	stop	start	stop															
	Inclusion Criteria:							>500	>2.0	>1.1									
Chromosome 1																			
Excluded	29541369	29542779	29484524	29485934	Gm5525				NPA									Pseudogene	
Excluded	29986917	29987498	29930072	29930653	Gm7858				NPA									Pseudogene	
Excluded	30775399	30776800	30718554	30719955	Gm9898				NPA									Predicted protein coding gene	
Excluded	30826532	30829182	30769687	30772337	Gm6473				NPA									Pseudogene	
Excluded	30846887	30858080	30790042	30801235	Gm2914				NPA									Pseudogene	
Yes	30859187	30920101	30802342	30863256	Phf3			14169.46	11942.00	1.70	1.05	29.71		1		2 T	N	Transcription	
					Phf3				11942.00	1.70	1.05	29.71		1		2 T	N	Transcription	
Excluded	38003583	38014604	37946738	37957759	Lyg1			28.54	27.71	1.15							EC	Glycoside hydrolase, extracellular	
Yes	38040712	38054053	37983867	37997208	Txndc9			11591.53	1474.89	2.13	5.23	29.60	3	2		1 E	C	Cell redox homeostasis	
					Txndc9				1474.89	2.13	5.23	29.60	3	2		1 E	C	Cell redox homeostasis	
Yes	38054855	38112424	37998010	38055579	Eif5b	+	+	4786.7594	7990.97	3.33	1.25	29.24	1	1		3 E	C	Translation	
					Eif5b				7990.97	3.33	1.25	29.24	1	1		3 E	C	Translation	
Excluded	38109631	38186507	38052786	38129662	Rev1		+	1758.06	5019.75	1.76	1.08	28.62		0		0	N	DNA repair	
Yes	38234172	38721800	38177327	38664955	Aff3			1367.95	1312.82	2.20	1.71	33.71		0		0 T	N	Transcription	
Excluded	38851354	38878060	38794509	38821215	Lonrf2			290.69	683.28	1.78				0				C	Peptidase
Excluded	38920717	38955005	38863872	38898160	Chst10			43.52	51.42	1.24						E	C	Carbohydrate metabolism	
Excluded	38941599	38946978	38884754	38890133	Gm19877				NPA									Non coding RNA	
Excluded	38964771	38965590	38907926	38908745	Gm6621				NPA									Pseudogene	
Excluded	38995994	39007121	38939149	38950276	Nms				NPA									EC	Neuropeptide signaling
Yes	39044659	39054081	38987814	38997236	Pdcl3		+	5312.23	5442.22	1.11	1.46	28.56	1	2		13 A	C	Apoptosis	
Yes	39251117	39420085	39194272	39363240	Npas2			750.72	633.69	1.44	2.74	32.08		0		0 T	N	Transcription, circadian rhythm	
Excluded	39335422	39337873	39278577	39281028	Gm17904				NPA									Pseudogene	
Excluded	39371709	39372331	39314864	39315486	Gm3617				NPA									Pseudogene	
Excluded	39424696	39428756	39367851	39371911	Rpl31		+	1596.4	669.70	1.20				0		0	C	Ribosomal protein	
Yes	39428340	39535592	39371495	39478747	Tbc1d8			3994.77	6536.65	1.41	1.11	28.58		0		0 G	C	Regulation of GTPase activity	
Yes	39592647	39603726	39535802	39546881	D1Bwg0212e		+	13931.98	12407.33	1.13	1.22	27.48		0		0 R	C	Possible mRNA deadenylation	
					D1Bwg0212e		+		12407.33	1.13	1.22	27.48		0		0 R	C	Possible mRNA deadenylation	
Excluded	39605592	39605685	39548747	39548840	Snord89			13.3	14.55	1.20						R	N	Small nuclear RNA	
Excluded	39607114	39607690	39550269	39550845	Gm18446				NPA									Pseudogene	
Yes	39608141	39634192	39551296	39577347	Rnf149			207.74	594.69	2.24	3.02	33.35		0		0	M	Membrane protein, ubiquitination	
Excluded	39654258	39654851	39597413	39598006	Gm5100				NPA									Pseudogene	
Excluded	39675251	39708027	39618406	39651182	Creg2			44.49	62.47	1.22						ER/PT	ER,EC	Brain glycoprotein	
Excluded	39722146	39777834	39665301	39720989	Rfx8			39.1	44.42	1.16						T	N	DNA binding	
Excluded	39860986	39862177	39804141	39805332	Gm3646				NPA									Predicted protein coding gene	
Excluded	unlisted	unlisted	39842428	39847330	1700066B17Rik				NPA									Noncoding RNA	
Excluded	39957758	40083155	39900913	40026310	Map4k4			649.84	567.35	1.25				0		0	C	Negative regulation of glucose transport	
Excluded	40133073	40142696	40076212	40085851	Gm16894				NPA									lincRNA	
Excluded	40141613	40182070	40084768	40125225	Il1r2			1413.53	655.02	1.29				0		0	M	Interleukin receptor, inhibitor of IL1 function	
Excluded	40281925	40373022	40225080	40316177	Il1r1			1751.11	2500.30	1.68								M	Interleukin receptor
Excluded	40381472	40422316	40324627	40365471	Il1r2			42.36	44.03	1.02								M	Interleukin receptor
Excluded	40410706	40411452	40353861	40354607	Gm17970				NPA									Pseudogene	
Excluded	40496494	40522260	40439649	40465415	Il1r1			98.84	101.55	1.33								M	Interleukin receptor
Excluded	40522397	40557699	40465552	40500854	Il18r1			17.66	18.90	1.14								M	Interleukin receptor
Excluded	40572207	40606148	40515362	40549303	Il18rap			141.6	139.91	1.18								M	Interleukin receptor
Excluded	40637072	40687576	40580227	40630731	Slc9a4			97.13	171.98	1.54				0		0	M	Sodium.hydrogen exchanger	

Excluded	40738557	40825730	40681712	40768885	Slc9a2			29.9	35.15	1.17				M	Sodium.hydrogen exchanger	
Yes	40828885	40847502	40772040	40790657	Mfsd9			1714.92	3085.72	1.16	1.41	31.32	0	0	M	Membrane transport
Yes	40862446	40912112	40805601	40855267	Tmem182			2572.21	2668.59	2.24	3.27	34.73	0	0	M	Endosome/lysosome
					Tmem182				2668.59	2.24	3.27	34.73	0	0	M	Endosome/lysosome
Excluded	40920384	40921084	40863539	40864239	Gm5973			NPA								Pseudogene
Excluded	unlisted	unlisted	41167560	41181252	4930448I06Rik			NPA		not detected						Non-coding RNA,expressionreported for testis
Excluded	42160006	42161394	42103161	42104549	Gm5267			NPA								Pseudogene
Excluded	42236128	42237233	42179283	42180388	Gm8176			NPA								Pseudogene

Chromosome 4

Excluded	6614533	6917870	6687386	6990723	Tox			164.26	272.39	1.13	1.19	33.60	0	0	T	N	DNA binding, transcription, thymocyte selection
Excluded	unlisted	unlisted	7560688	7573801	8430436N08Rik			44.89	50.00	1.11							lincRNA gene
Yes	8068640	8166188	8141493	8239041	Car8			1142.82	672.88	9.16	7.16	32.27	0	2	E	C	Inhibits binding IP3 to ITPR1
					Car8				672.88	9.16	7.16	32.27	0	2	E	C	Inhibits binding IP3 to ITPR1
Excluded	8383313	8383645	8456166	8456498	Gm11810			NPA									Pseudogene
Excluded	8388639	8394627	8461492	8467480	Gm18098			NPA									Pseudogene
Yes	8462791	8534849	8535644	8607702	Rab2a			5143	7209.38	1.44	1.16	31.14	0	0	ER/PT	ER	Protein transport from ER
Excluded	8574111	8574694	8646964	8647547	Gm8273			NPA									Unclassified putative gene
Excluded	8599783	8600729	8672636	8673582	Gm11809			NPA									Pseudogene
Yes	8618068	8793957	8734909	8866810	Chd7			5582.05	13263.50	1.43	1.39	31.27	0	0	T	N	Transcription, chromatin remodeling, regulation of pluripotency
					Chd7				13263.50	1.43	1.39	31.27	0	0	T	N	Transcription, chromatin remodeling, regulation of pluripotency
Excluded	8868406	8868842	8941259	8941695	Rps18-ps2			NPA									Pseudogene
Excluded	9196464	9378838	9269317	9451691	Clvs1			1155	620.23	1.71			0	0	ER/PT	V	Retinaldehyde binding
Yes	9376232	9596309	9449085	9669162	Asph			1035.38	828.26	1.54	1.35	29.71	3	3	ER/PT	ER	Hydroxylation of EGF-like domains; regulation of calcium transport
Excluded	9497110	9497640	9569963	9570493	Gm19130			NPA									Pseudogene
Excluded	9697732	9750558	9770585	9823411	4930412C18Rik			116.36	197.50		2.01						lincRNA gene
Excluded	9771519	9789492	9844372	9862345	Gdf6			NPA								EC	BMP signaling
Excluded	9843112	9844544	9915965	9917397	4930448K20Rik			114.51	169.94		1.39						Pseudogene
Excluded	10365482	10366987	10438335	10439841	Gm11814			NPA									Pseudogene
Excluded	unlisted	unlisted	10508031	10797802	1700123O12Rik			77.76	79.72		1.36						lincRNA gene
Excluded	10740676	10741919	10813529	10814772	Gm12920			NPA									Pseudogene
Excluded	unlisted	unlisted	10845500	10845630	Mir3471-1			NPA									MicroRNA
Excluded	10775567	10776240	10848387	10849110	Gm12918			NPA									Pseudogene
Excluded	10780990	10782580	10853714	10855633	Gm12919			NPA									Pseudogene
Excluded	10801211	10801292	10874064	10874145	Trnas-aga			NPA							ER/PT	ER	Asparagine catabolism
Excluded	10801645	10826572	10874498	10899425	2610301B20Rik			26.09	28.36		1.09						protein coding gene
Excluded	10873755	10874217	10946608	10947070	Gm11828			NPA									Pseudogene
Excluded	10914477	10917462	10987330	10990315	Gm2401			NPA									Pseudogene
Excluded	10915809	10934766	10988662	11007619	Plekht2			108.79	87.62		1.07				ER/PT	V	Phospholipid binding, vesicle transport
					Ndufaf6/2310030												
Excluded	10978192	11003351	11051045	11076204	N02Rik			1166.42	153.96		2.05					MT	Mitochondrion
Excluded	11049952	11054145	11122805	11126998	Gm11827			NPA									lincRNA gene
Excluded	11060365	11060953	11133218	11133806	Gm11829			NPA									Pseudogene
Excluded	11061244	11061329	11134097	11134182	Mir684-2			NPA									MicroRNA
Excluded	11083588	11101524	11156441	11174377	Trp53inp1			6145.59	9606.89	1.45	1.06	28.77	0	0	T,A	N	Apoptosis, stress response
Yes	11118501	11131926	11191354	11204779	Ccne2			490.92	594.62	4.15	2.36	32.43	1	2			Cell cycle
Yes	11126305	11181406	11199158	11254259	Ints8			1215.38	2404.63	1.58	1.18	30.91	0	1	R	N	snRNA processing
Yes	11192226	11249278	11265079	11322131	Dpy19I4			1399.6	2677.87	3.78	1.15	32.49	1	0		M	Membrane
Excluded	unlisted	unlisted	11318074	11332923	LOC100861935			NPA									
Yes	11259185	11313930	11332038	11386783	Esrp1			9379.61	10115.00	1.15	1.17	27.23	1	2	R	N	mRNA splicing
Excluded	11327238	11328471	11400091	11401324	Gm11821			Y. c	NPA	al.							
Excluded	11347193	11348004	11420046	11420857	Gm20012			NPA									
Yes	11413105	11478290	11485958	11551143	1110037F02Rik			4024.29	6792.12	1.34	1.61	29.56	1	1	R	N	mRNA processing
Excluded	11486119	11542954	11558920	11615808	Rad54b			1404.84	155.16		1.32		0	0			Recombinational repair DNA damage

Excluded	11506809	11514964	11579662	11587802 Fsbp	NPA													Fibrinogen silencer binding protein	
Excluded	11576760	11577677	11649613	11650530 Gm11833	NPA													Pseudogene	
Excluded	11631594	11642140	11704447	11714993 Gem	23.69	24.49	1.30											GTP signaling	
Yes	11685304	11745052	11758157	11817905 Cdh17	5582.05	157.82	2.64	2.61	31.38	0	0			M			Cell adhesion		
Excluded	11885332	11893597	11958185	11966450 Pdp1	1496.84	2764.67	1.25											Mitochondrion Protein, reactivation pyruvate dehydrogenase	
Excluded	11893712	11921442	11966574	11994295 1700123M08Rik	NPA													lincRNA gene	
Excluded	11906707	11908412	11979560	11981265 Gm10604	NPA														
Excluded	11966502	12015104	12039355	12087957 Tmem67 Rbm12b2/C43004	32.56	35.04	1.11										M	Cell projection morphogenesis	
Excluded	12016517	12023418	12089370	12096271 8L16Rik	208.24	435.94	1.87									R		RNA binding	
Excluded	12041231	12043585	12114084	12116438 Gm11839	NPA													Pseudogene	
Excluded	12052237	12054596	12125090	12127449 Gm11841	NPA													Pseudogene	
Excluded	12058698	12059122	12131551	12131975 Gm11843	NPA													Pseudogene	
Excluded	12067264	12073892	12140117	12146745 Rbm12b	163.73	421.29	1.81											RNA binding	
Excluded	12080869	12099162	12153722	12172015 Fam92a	12.82	1181.14	1.22											protein coding gene	
Excluded	12159927	12161837	12232772	12238024 Gm11847	NPA													Pseudogene	
Excluded	12833984	12908632	12906837	12981485 Gm11818	NPA			1.09	30.80									lincRNA gene	
Excluded	13371910	13374740	13444763	13447593 Gm20032	NPA													Pseudogene	
Excluded	13409709	13410340	13482562	13483193 Gm11826	NPA													Pseudogene	
Yes	13670449	13820796	13743302	13893649 Runx1t1	2812.23	6410.87	2.00	1.37	31.31	0	0			T		N		Pluripotency, transcription	
Chromosome 17																			
Excluded	66686322	66799090	66336982	66449750 Soga2/111001217Rik	109.8	114.69	1.64											protein coding gene	
Excluded	66762971	66763324	66413631	66413995 Gm4705	NPA													protein coding gene	
Excluded	66843852	66869010	66494512	66519670 Rab12 Themis3/9130404	685.57	1620.02	1.12											Transferrin receptor degradation	
Excluded	66904592	66943962	66555252	66594622 H23Rik	312.41	1038.91	1.71										M	Cell adhesion	
Excluded	67016188	67703799	66666848	67354459 Ptprm	163.03	301.81	1.25										M	Cell adhesion	
Excluded	67172460	67173120	66823120	66823780 Gm18961	NPA													Pseudogene	
Excluded	67359825	67368732	67010485	67019392 Gm9984	NPA													unclassified gene	
Excluded	67980305	67982063	67630965	67632723 Lrrc30	NPA													unknown	
Excluded	68046605	68171985	67697265	67822645 Lama1	188.46	87.02	1.16										EC	Extracellular matrix	
Yes	68192046	68353448	67842706	68004108 Arhgap28	3788.58	6561.93	1.53	13.87	30.97	0	1						C,N	Rho GTPase activation, signaling	
Yes	68192046	68353448	67842706	68004108 Arhgap28	3788.58	6561.93	1.53	13.87	30.97	0	1							C,N	Rho GTPase activation, signaling
Poor																		Poor	
Detection	68623137	69129426	68273797	68780086 L3mbtl4	NPA													T	Chromatin modification, transcription
Excluded	68720626	68721212	68371286	68371872 Gm15974	NPA														Pseudogene
Excluded	69048251	69049667	68698911	68700327 Gm17921	NPA														Pseudogene
Excluded	69506150	69639329	68837136	68843138 Tmem200c	79.94	88.31	1.18												
Yes	69506150	69639329	69156810	69289989 Epb4.113	545.67	1056.10	1.78	2.68	35.47	0	0							CSK	Actin cytoskeleton, Ezrin/Radixin?Moesin domain containig, regulator of proliferation and apoptosis
Excluded	unlisted	unlisted	69275362	69277206 2410021H03Rik	1056.10	1.78	2.68	35.47	0	0								CSK	Actin cytoskeleton, Ezrin/Radixin?Moesin domain containig, regulator of proliferation and apoptosis
Yes	69733318	69739884	69733318	69739884 Zfp161	1097.03	878.10	1.36	1.47	35.78	0	0							T	Transcription, Myc repressor
Excluded	unlisted	unlisted	69386406	69390545 LOC100861864	NPA														
Excluded	69765787	69768533	69416447	69419193 C030034122Rik	18.41	22.51	1.35												Non-coding RNA melanocyte cDNA, expression reported in ovary, embryonic day 2, and postnatal life
Excluded	69788666	69838573	69439326	69489233 A330050F15Rik	164.58	186.19	1.14												protein coding gene; RNA expression reported in brain, medulla, spinal cord
Excluded	69903564	69904124	69554224	69554784 Gm9319	NPA														Pseudogene
Excluded	69919742	69920521	69570402	69571181 Gm9598	NPA														Pseudogene
Excluded	70274667	70275171	69925327	69925831 Gm4561	NPA														Pseudogene
Excluded	70741937	70742895	70392597	70393569 Stmn1-rs2	NPA														Pseudogene
Excluded	70749474	70750114	70400134	70400774 Gm6399	NPA														Pseudogene

10 SI

Y. C. al.

Yes	70774132	71170753	70424792	70821413	Dlgap1			245.16	465.93	1.56	6.49	32.80	0	3	M	Channel clustering	
Yes	71193545	71202872	70844205	70853532	Tgif1			208.1	108.74	1.11	1.38	35.22	0	1	T	N	Chromatin binding
Yes	71193545	71202872	70844205	70853532	Tgif1			208.1	108.74	1.11	1.38	35.22	0	1	T	N	Chromatin binding
Excluded	71203108	71225581	70853768	70876241	Gm9320			NPA								Pseudogene	
Excluded	unlisted	unlisted	70860478	70860600	Mir1195			NPA								MicroRNA	
Excluded	71278398	71278886	70929058	70929546	Gm16519			NPA								predicted protein coding gene	
Excluded	71306464	71307260	70957099	70957920	Gm4947			NPA								predicted gene	
Deferred	71323303	71339856	70973963	70990516	Myl12b			1307.66	2067.50	1.30			1	3	CSK	Myosin contractility	
Deferred	71343133	71351873	70993793	71002533	Myl12a			8339.09	9578.09	1.38	1.29	30.11	1	2	M	Myosin, glutamate receptor binding, cell shape related	
Excluded	unlisted	unlisted	70994294	71001873	LOC100861887			NPA									
Excluded	71368897	71476196	71019557	71126856	Myom1			103.98	55.93	1.42					CSK	Muscle contraction	
Yes	71533318	71599158	71183978	71249818	Lpin2	+	+	13590.61	12641.53	1.24	1.68	29.79	0	0	E		Fatty acid metabolism
Excluded	71601516	71660305	71252176	71310965	Emilin2			3445.36	1106.94	1.29			1	3	M	Cell adhesion	
Excluded	unlisted	unlisted	71315456	71339746	4930471L23Rik			NPA								non-coding RNA, expression adult tissues	
Excluded	71682541	71691144	71333201	71341804	Gm4566			NPA								Pseudogene	
Yes	71693829	71824683	71344489	71475343	Smchd1	+		2501.88	3999.78	1.36	1.69	33.29	1	0	T	N	X chromosome inactivation
Excluded	71832709	71833263	71458178	71459899	LOC100534390			NPA								X chromosome inactivation	
Excluded	unlisted	unlisted	71483369	71483923	Gm18738			NPA								Pseudogene	
Yes	71845440	71876197	71496100	71526857	Ndc80			1942.97	3718.72	2.15	4.23	32.12	2	0	E	CSK	Kinetochores, required in early embryos
Excluded	71878326	71893547	71528986	71544207	Mettl4-ps1			11.45	11.18	1.11						Pseudogene	
Excluded	71901401	71938873	71552061	71589533	Spdy4			21.74	17.80	1.04					CSK	Cell cycle	
Excluded	71906367	71948101	71557027	71598761	Trmt61b			38.99	47.12	1.31						tRNA methyltransferase	
Excluded	71919126	71919759	71569786	71570419	Gm18140			NPA								Pseudogene	
Excluded	71948611	71948682	71599271	71599342	Trnac-gca			24.12	32.42	20.33					C	cytoplasm, calcium dependent localization to granules	
Excluded	71965555	72008371	71616215	71659031	Wdr43			4416.92	1858.97	1.19			0	0	C	Protein processing	
Excluded	71980631	71980701	71631279	71631361	Snord92			NPA								N	Small nucleolar RNA
Excluded	71990229	71990296	71640889	71640956	Snord53			NPA								N	Small nucleolar RNA
Excluded	72022601	72079009	71673261	71729669	Fam179a			171.67	188.34	1.05			0	0		protein coding gene	
Excluded	72092895	72102225	71743555	71752885	BC027072			44	46.51	1.23						protein coding gene	
Yes	72119031	72207691	71769691	71858351	Clip4			2362.88	4983.50	1.24	1.34	30.86	0	0	E	M	Regulator of endocytosis
Excluded	72218328	72953647	71868988	72604307	Alk			176.41	223.83	1.63			0	3	M	growth regulator, nervous system development	
Excluded	unlisted	unlisted	72256258	72257143	Gm19183			NPA								Pseudogene	
Excluded	72605598	72606483	72699458	72700445	LOC100861994			NPA								Pseudogene	
Yes	73186044	73200535	72836704	72851195	Ypel5			16725.19	20242.68	1.09	1.39	28.95	3	2	E	C	cell cycle, stem cell fate and expansion
Excluded	73267645	73291286	72918305	72941946	Lbh			197.18	252.13	1.04			0	1	T	N	Transcription
Yes	73457325	73592708	73107985	73243368	Lclat1			564.23	1206.55	5.52	1.51	32.52	0	1	ER/PT	ER	Phospholipid remodeling in ER
Excluded	73539598	73541025	73190258	73191349	Gm9311			NPA								Pseudogene	
Excluded	73655804	73748636	73306464	73399296	Capn13			42.14	41.22	1.07							
Excluded	73843091	74059791	73493751	73710451	Galnt14			58.32	44.16	1.23							
Excluded	74154181	74181433	73804841	73832093	Ehd3			516.48	310.92	1.32			2	1	ER/PT	V	Endocytic recycling
Excluded	74219665	74220786	73870325	73871446	Gm4948			NPA								Pseudogene	
Poor detection	74233248	74299522	73883908	73950182	Xdh			2942.83	1924.20	3.45	Poor detection		0	0			
Excluded	74282595	74283238	73933255	73933898	Gm18068			NPA								Pseudogene	
Excluded	74367046	74397256	74017706	74047916	Srd5a2			43.57	34.62	1.20					C	androgen biogenesis	
Deferred	74600040	74694203	74200700	74294863	Memo1	+		3752.88	3482.83	1.25					CSK	Regulation of cell motility	
Excluded	74611078	74613615	74211738	74214275	Gm9316			NPA								Pseudogene	
Yes	74698814	74723284	74299474	74323944	Dpy30	+	+	9086.81	13401.76	1.20	1.11	27.84	0	0	T	N	Histone methyltransferase complex
Excluded	74728618	74729241	74329278	74329901	Gm9349			NPA								Pseudogene	
Excluded	74731303	74731889	74331963	74332549	Gm9351			NPA								Pseudogene	
Yes	74738327	74790453	74338987	74391113	Spast	+	+	7394.17	1023.36	3.10	1.74	31.57	0	0		CSK	Regulation of microtubule function, organelle dis
Excluded	74794972	74823569	74395608	74424229	Slc30a6			187.21	39.04	1.50			0	0		CSK	Regulation of microtubule function, organelle dis
Excluded																M	Zinc transport

Excluded	74825635	74858448	74426295	74459108	Nlrc4														A	Apoptosis
Excluded	74837625	74837979	74438285	74438639	Gm4708															Pseudogene
Excluded	74886611	74887361	74487271	74488021	Gm6476															Pseudogene
Yes	74888854	74899617	74489493	74500277	Yipf4														0 ER/PT	ER
Excluded	74927635	75103113	74528295	74703773	Birc6														1 A	CSK
Excluded	75117090	75262910	74717750	74863570	Ttc27														0	
Excluded	75404869	75791109	75005529	75392967	Ltbp1															EC
Excluded	75564516	75565200	75165176	75165860	Gm6276															Pseudogene
Excluded	75835245	75928394	75435905	75529054	Rasgrp3															G
Excluded	75936426	75951286	75537086	75551946	Fam98a															C
Excluded	76060480	76062055	75661127	75662715	Gm9360															
Excluded	76260363	76288379	75861023	75889039	Gm4710															

Inclusion Criteria to select genes for expression analysis: Combination of at least 500 maximum raw intensity value on array; at least 2-fold change on array; at least 10% change in qRT-PCR; and relevance of biofunction and cell compartment characteristics. Excluded if no detection on MII oocyte arrays. Excluded extracellular and secreted products and pseudogenes. Lower priority assigned to membrane proteins. Micro RNAs were excluded because oocytes and early embryos do not employ miRNAs for gene regulation. Highest biofunction and cell compartment priorities assigned as shown in column L. NPA, no probe on array

Biofunction Definitions: A, apoptosis; C, cytoplasm; CSK, cytoskeleton; E, embryonic role, EC, extracellular; ER/PT, ER or protein transport; FA, fatty acid metabolism; G, GTPase signaling; M, membrane MT, mitochondria; N, nucleus; R, RNA binding or processing; V, vesicle; T, transcription

Columns B-C, bold font indicates regions attaining significance in the interval mapping analysis

Column D colors reflect results of univariate analysis of correlation between expression and traits

* Oocyte proteome data of Wang et al., 2010. Proteome of mouse oocytes at different developmental stages. Proc Natl Acad Sci U S A. ;107:17639-44.

Bold Font denotes loci lying with the intervals with significant LRS based on build 37 as disclosed by GeneNetwork.org












	Correlation of expression with with 3 or 4 traits SCNT results 28 BXD strains without B6,D2, and B6D2 F1 genotypes
	Correlation of expression with with 2 traits SCNT results 28 BXD strains without B6,D2, and B6D2 F1 genotypes
	Correlation of expression with with 1 trait SCNT results 28 BXD strains without B6,D2, and B6D2 F1 genotypes
	Correlation with 1 or more additional traits based on SCNT development/parthenote developmental rates 28 strains without B6,D2, and B6D2 F1 genotypes
	Correlation of expression with 2 traits SCNT results using 28 strains with B6,D2, and B6D2 F1 genotypes
	Correlation with 3 or 4 traits using 28 BxD strains with B6,D2, and B6D2 F1 genotypes
	Correlation of expression with 1 trait SCNT results using 28 strains with B6,D2, and B6D2 F1 genotypes
	Correlation of expression with 1 trait using 6 BxD strains without B6,D2, and B6D2 F1 genotypes
	Criteria for excluding genes from further consideration
	Possible biofunction relevance
	Criteria for including genes for further consideration

Table S6. Single gene correlations for 6 selected BxD strains

				Pearson Correlation Coefficients and p values*											
				SCNT Trait				SCNT:Parthenote Trait				Parthenote Trait			
				2cell/ constr	4cell/ 2cell	Blast./ 2cell	Blast./ 4cell	2cell/ constr	4cell/ 2cell	Blast./ 2cell	Blast./ 4cell	2cell/ constr	4cell/ 2cell	Blast./ 2cell	Blast./ 4cell
With B6, D2 and B6D2 F1 Data															
Chrm 1															
start	stop	Symbol	Description												
	30802342	30863256 Phf3	PHD finger protein 3									-0.51427			
					0.79799	0.69515	0.73171			0.55803	0.47857	0.0061	0.87632	0.54374	0.53004
	37983867	37997208 Txndc9	thioredoxin domain containing 9		<.0001	<.0001	<.0001			0.0025	0.0116		<.0001	0.0034	0.0045
					0.55542	0.45879	0.46682	0.43894					0.62347	0.39281	
	37998010	38055579 Eif5b	eukaryotic translation initiation factor 5B		0.0026	0.0161	0.0141	0.0220					0.0005	0.0427	
	38177327	38664955 Aff3	AF4/FMR2 family, member 3							0.57314	0.57018		0.39659		
										0.0018	0.0019		0.0405		
	38987814	38997236 Pdc13	phosducin-like 3									-0.52372			
												0.0051			
	39194272	39363240 Npas2	neuronal PAS domain protein 2									0.39768			
												0.0400			
	39371495	39478747 Tbc1d8	TBC1 domain family, member 8							-0.39433		-0.46481			
			DNA segment, Chr 1, Brigham & Women's Genetics	0.54526	0.42849			0.75815		0.0418		0.0146		0.57674	0.57217
	39535802	39546881 D1Bwg0212e	0212 expressed	0.0033	0.0258			<.0001						0.0016	0.0018
												0.59348			
	39551296	39577347 Rnf149	ring finger protein 149									0.0011			
	40772040	40790657 Mfsd9	major facilitator superfamily domain containing 9									-0.44512			
					0.40025			0.55499				0.0200			
	40805601	40855267 Tmem182	transmembrane protein 182		0.0386			0.0027							
Chrm 4															
start	stop	Symbol	Description												
	8535644	8607702 Rab2a	RAB2A, member RAS oncogene family			-0.41243	-0.43337			-0.47924	-0.46167		-0.38416		
						0.0325	0.0239			0.0114	0.0153		0.0479		
	8734909	8866810 Chd7	chromodomain helicase DNA binding protein 7		-0.57875	-0.43826	-0.39121			-0.44731			-0.52856		
					0.0016	0.0222	0.0436			0.0193			0.0046		
	9449085	9669162 Asph	aspartate-beta-hydroxylase									-0.53583			
												0.0040			
	11191354	11204779 Ccne2	OTTMUSP00000004879	0.39925		0.38173	0.43945					0.52896			
				0.0391		0.0494	0.0218					0.0046			
	11199158	11254259 Ints8	integrator complex subunit 8					0.38372							
								0.0482							
	11265079	11322131 Dpy19l4	dpy-19-like 4 (C. elegans)		-0.42825					-0.40054	-0.38834				
					0.0258					0.0384	0.0453				
	11332038	11386783 Esrp1	epithelial splicing regulatory protein 1		-0.59975	-0.45534	-0.46206						-0.58127		
		1110037F02Ri			0.0009	0.0170	0.0152				0.0175		0.0015		
	11485958	11551143 k	RIKEN cDNA 1110037F02 gene							-0.50023					
										0.0079					
	11758157	11817905 Cdh17	cadherin 17									-0.46869			
												0.0137			
	13743302	13893649 Runx1t1	run-related transcription factor 1; translocated to, 1 (cyclin D-related)							-0.47839	-0.43276	-0.38229			
										0.0116	0.0242	0.0491			

9449085	9669162	Asph	aspartate-beta-hydroxylase					-0.65436	-0.59232	-0.47224				
				0.52567				0.0032	0.0096	0.0478				
11191354	11204779	Ccne2	OTTMUSP00000004879	0.0251				0.70482		0.66129				
								0.0011		0.0028				
11199158	11254259	Ints8	integrator complex subunit 8					0.55917						
								0.0158						
11265079	11322131	Dpy1914	dpy-19-like 4 (C. elegans)					-0.47973	-0.60695	-0.54008	-0.61714			
								0.0439	0.0076	0.0207	0.0064			
11332038	11386783	Esrp1	epithelial splicing regulatory protein 1	-0.56664				-0.55721	-0.62251		-0.70152			
				0.0142				0.0163	0.0058		0.0012			
11485958	11551143	k	RIKEN cDNA 1110037F02 gene					-0.56188	-0.48283		-0.55277			
								0.0152	0.0424		0.0174			
11758157	11817905	Cdh17	cadherin 17							0.52169				
										0.0264				
13743302	13893649	Runx1t1	runt-related transcription factor 1; translocated to, 1 (cyclin D-related)						-0.60838	-0.61151				
									0.0074	0.0070				
Chrm 17														
start	stop	Symbol	Description											
					0.51934	0.48102		-0.54042			0.49192	0.47163		
67842706	68004108	Arhgap28	Rho GTPase activating protein 28		0.0272	0.0433		0.0206			0.0381	0.0482		
69156810	69289989	Epb4.1l3	erythrocyte protein band 4.1-like 3	-0.81138	-0.54815	-0.53809			-0.71092		-0.76646			
				<0.0001	0.0185	0.0212			0.0009		0.0002			
69383978	69390544	Zfp161	zinc finger protein 161									0.54331	0.52477	
												0.0198	0.0254	
70424792	70821413	Dlgap1	discs, large (Drosophila) homolog-associated protein 1					-0.55587		0.56344	0.50316			
								0.0166		0.0149	0.0333			
70844205	70853532	Tgif1	TGFB-induced factor homeobox 1	-0.54742				-0.57461						
				0.0187				0.0126						
71183978	71249818	Lpin2	lipin 2							-0.50953				
					0.68740	0.48232	0.48303			0.0308				
71344489	71475343	Smchd1	SMC hinge domain containing 1		0.0016	0.0426	0.0423			0.75620	0.50750	0.64905		
					0.68904	0.93648	0.84663	0.83574	0.65856	0.0003	0.0316	0.0036		
71496100	71526857	Ndc80	NDC80 homolog, kinetochore complex component (S. cerevisiae)	0.0016	<0.0001	<0.0001	<0.0001	0.0030			0.53985	0.91805	0.83955	0.84290
					-0.72749	-0.54458	-0.52689				0.0207	<0.0001	<0.0001	<0.0001
72836704	72851195	Ypel5	yippee-like 5 (Drosophila)		0.0006	0.0195	0.0247		-0.65846		-0.57554	-0.61166		
					0.82219			0.82320	0.0030		0.0124	0.0070		
73107985	73243368	Lclat1	lysocardiolipin acyltransferase 1	<0.0001				<0.0001			0.57353			
					-0.50194						0.0128			
74299474	74323944	Dpy30	dpy-30 homolog (C. elegans)		0.0338				-0.47306					
					0.76139	0.81293	0.80349		0.0474					
74338987	74391113	Spast	spastin		0.0002	<0.0001	<0.0001					0.81864	0.80954	0.81426
												<0.0001	<0.0001	<0.0001

* a (-) sign denotes a negative correlation between delta CT value and the trait, which indicates a positive association between mRNA expression and the trait. Blast. Denotes blastocyst.

Results are shown for testing correlations of expression of 36 genes (see first column Table S5) on six selected BxD strains. Correlations were tested with and without parental strain data included. Data for significant correlations are shown. Map coordinates are from build 38.

Table S7. Single gene correlations for 28 BxD strains

				Pearson Correlation Coefficients and p values*											
				SCNT Trait				SCNT:Parthenote Trait				Parthenote Trait			
				2cell/ constr	4cell/ 2cell	Blast./ 2cell	Blast./ 4cell	2cell/ constr	4cell/ 2cell	Blast./ 2cell	Blast./ 4cell	2cell/ constr	4cell/ 2cell	Blast./ 2cell	Blast./ 4cell
With B6, D2 and B6D2 F1 Data															
Chrm 1															
start	stop	Symbol	Description												
				0.24310				0.42896		-0.28292				-0.26616	
30802342		30863256 Phf3	PHD finger protein 3	0.0189				<0.0001		0.0060				0.0099	
				0.44113	0.39629	0.37285				-0.26282			0.45164	0.41846	0.45000
37983867		37997208 Txndc9	thioredoxin domain containing 9	<0.0001	<0.0001	0.0002				0.0109			<0.0001	<0.0001	<0.0001
				0.51592	0.52420	0.28254							0.35634	0.31360	0.22838
37998010		38055579 Eif5b	eukaryotic translation initiation factor 5B	<0.0001	<0.0001	0.0061							0.0005	0.0022	0.0277
						0.39965							0.28935		
38177327		38664955 Aff3	AF4/FMR2 family, member 3			<0.0001							0.0049		
															-0.21791
38987814		38997236 Pdc13	phosducin-like 3												0.0359
						0.26992									
39371495		39478747 Tbc1d8	TBC1 domain family, member 8			0.0089									
						0.21489				-0.36501			0.39935	0.38786	0.33304
39535802		39546881 D1Bwg0212e	DNA segment, Chr 1, Brigham & Women's Genetics 0212 expressed			0.0386				0.0003			<0.0001	0.0001	0.0011
										-0.24590	0.29150	0.42721			
40772040		40790657 Mfsd9	major facilitator superfamily domain containing 9							0.0175	0.0046	<0.0001			
						0.26402							0.26730	0.27513	0.31339
40805601		40855267 Tmem182	transmembrane protein 182			0.0106							0.0096	0.0076	0.0022
Chrm 4															
start	stop	Symbol	Description												
						0.45127	0.21152			0.32255					-0.26851
8141493		8239041 Car8	carbonic anhydrase 8			<0.0001	0.0418			0.0016					0.0093
						-0.26988	-0.26209								
8535644		8607702 Rab2a	RAB2A, member RAS oncogene family			0.0089	0.0112								
						-0.24082				-0.23309	0.22034	0.29044			
8734909		8866810 Chd7	chromodomain helicase DNA binding protein 7			0.0201				0.0245	0.0338	0.0047			
										-0.22288	-0.32703	-0.21849		0.33239	0.23833
9449085		9669162 Asph	aspartate-beta-hydroxylase	-0.21785						0.0318	0.0014	0.0354		0.0011	0.0214
				0.0359										0.35053	0.38511
11191354		11204779 Ccne2	OTTMUSP00000004879	0.26512			0.34479			-0.40626	-0.24847		0.0006	0.0001	0.0014
				0.0102			0.0007			<0.0001	0.0163		0.0006	0.0001	0.0014
															0.0471
11265079		11322131 Dpy19l4	dpy-19-like 4 (C. elegans)												-0.23169
															0.0254
11332038		11386783 Esrp1	epithelial splicing regulatory protein 1			-0.30625	-0.24632			-0.21833	-0.33302				
						0.0028	0.0173			0.0355	0.0011				
13743302		13893649 Runx11	runt-related transcription factor 1; translocated to, 1 (cyclin D-related)												-0.21511
															0.38528
															0.0001
Chrm 17															
start	stop	Symbol	Description												
						0.48531	0.35766	0.21717		0.28736					
67842706		68004108 Arhgap28	Rho GTPase activating protein 28			<0.0001	0.0004	0.0365		0.0052					
						-0.36225	-0.22823					0.30477	0.24197		
69156810		69289989 Epb4.1l3	erythrocyte protein band 4.1-like 3			0.0004	0.0278					0.0030	0.0195		
							-0.23976								-0.22604
70424792		70821413 Dlgap1	discs, large (Drosophila) homolog-associated protein 1				0.0206							0.0294	
								0.25040		-0.34642				0.47703	0.34464
70844205		70853532 Tgif1	TGFB-induced factor homeobox 1					0.0155		0.0007				<0.0001	0.0007
						-0.23596	0.40904	0.26252							0.0110
						0.0228	<0.0001	0.0110	0.0448						
71344489		71475343 Smchd1	SMC hinge domain containing 1			-0.25619	0.34018	0.23719	0.23023					-0.30259	0.24320
						0.0132	0.0008	0.0221	0.0264				0.0032	0.0188	
71496100		71526857 Ndc80	NDC80 homolog, kinetochore complex component (S. cerevisiae)				-0.42550	-0.24220							
							<0.0001	0.0193		-0.40502	-0.27251				
72836704		72851195 Ypel5	yippee-like 5 (Drosophila)							<0.0001	0.0082				
								0.35675		-0.38170	-0.24774			0.28331	0.51871
73107985		73243368 Lclat1	lysocardiolipin acyltransferase 1	0.21979			0.0004			0.0002	0.0167		0.0059	<0.0001	<0.0001
				0.0343											0.0008

				0.29881	0.29516					-0.24208			
				0.0036	0.0041					0.0194			
Without B6, D2 and B6D2 F1 Data				2cell/cons	Blastocyst	Blastocyst	2cell/cons	Blastocyst	Blastocyst	2cell/cons	Blastocyst	Blastocyst	
				tr	4cell/2cell	/2cell	tr	4cell/2cell	/2cell	tr	4cell/2cell	/4cell	
Chrm 1													
start	stop	Symbol	Description										
30802342	30863256	Phf3	PHD finger protein 3				0.44218		-0.26292		-0.37136		
							<0.0001		0.0157		0.0005		
37983867	37997208	Txndc9	thioredoxin domain containing 9	0.38288	0.30550	0.33877			-0.28560		0.39725	0.43453	0.49622
				0.0003	0.0047	0.0016			0.0085		0.0002	<0.0001	<0.0001
37998010	38055579	Eif5b	eukaryotic translation initiation factor 5B	0.44303	0.50650	0.32570	0.22083				0.30433	0.39444	0.33589
				<0.0001	<0.0001	0.0025	0.0435				0.0049	0.0002	0.0018
38177327	38664955	Aff3	AF4/FMR2 family, member 3			0.41675					0.33060	0.23066	
						<0.0001					0.0021	0.0348	
38987814	38997236	Pdcl3	phosducin-like 3	-0.23886	-0.29621				0.21640		-0.22758	-0.22660	
				0.0287	0.0062				0.0480		0.0373	0.0382	
39371495	39478747	Tbc1d8	TBC1 domain family, member 8			0.26874							
						0.0134							
39535802	39546881	D1Bwg0212e	DNA segment, Chr 1, Brigham & Women's Genetics 0212 expressed		0.25547	0.27546			-0.35813		0.45217	0.43410	0.37277
					0.0190	0.0112			0.0008		<0.0001	<0.0001	0.0005
40772040	40790657	Mfsd9	major facilitator superfamily domain containing 9			0.26064					0.27754		
						0.0166	-0.25124	0.30760	0.43950		0.0106		
40805601	40855267	Tmem182	transmembrane protein 182	0.27254	0.36270	0.39486	0.0212	0.0044	<0.0001		0.38917	0.35572	0.38253
				0.0121	0.0007	0.0002					0.0003	0.0009	0.0003
Chrm 4													
start	stop	Symbol	Description										
8141493	8239041	Car8	carbonic anhydrase 8	0.60694	0.45625		0.34185		-0.28244				0.25838
				<0.0001	<0.0001		0.0015		0.0092				0.0176
8734909	8866810	Chd7	chromodomain helicase DNA binding protein 7										
								0.22307	0.27825				
9449085	9669162	Asph	aspartate-beta-hydroxylase	-0.25708			-0.29417	-0.37222	-0.23661		0.28904	0.27469	0.23224
				0.0182			0.0066	0.0005	0.0302		0.0077	0.0114	0.0335
11191354	11204779	Ccne2	OTTMUSP0000004879	0.26938		0.26382		-0.42332	-0.31064		0.34650	0.34458	0.29180
				0.0132		0.0153		<0.0001	0.0040		0.0012	0.0013	0.0071
11332038	11386783	Esrp1	epithelial splicing regulatory protein 1					-0.35610	-0.23641				
								0.0009	0.0304				
13743302	13893649	Runx11	runt-related transcription factor 1; translocated to, 1 (cyclin D-related)			0.22879				0.37555			
						0.0363				0.0004			
Chrm 17													
start	stop	Symbol	Description										
67842706	68004108	Arhgap28	Rho GTPase activating protein 28	0.61347	0.61803	0.34353	0.29694	0.22183					
				<0.0001	<0.0001	0.0014	0.0061	0.0426					
69156810	69289989	Epb4.1l3	erythrocyte protein band 4.1-like 3	-0.29662	-0.23106					0.26902	0.27487		
				0.0061	0.0345					0.0133	0.0114		
70424792	70821413	Dlgap1	discs, large (Drosophila) homolog-associated protein 1	0.45914	0.37485				0.22524				
				<0.0001	0.0004				0.0394				
70844205	70853532	Tgif1	TGFB-induced factor homeobox 1			0.22012	-0.21994	-0.38317			0.43766	0.32606	0.25695
						0.0442	0.0444	0.0003			<0.0001	0.0025	0.0183
71344489	71475343	Smchd1	SMC hinge domain containing 1	0.51953	0.48103	0.31112		0.21810			0.26277		
				<0.0001	<0.0001	0.0040		0.0463			0.0157		
71496100	71526857	Ndc80	NDC80 homolog, kinetochore complex component (S. cerevisiae)	-0.25716	0.44753	0.48822			0.27020		-0.29553	0.36915	
				0.0182	<0.0001	<0.0001			0.0129		0.0063	0.0005	
72836704	72851195	Ypel5	yippee-like 5 (Drosophila)	-0.47460	-0.35484			-0.40608	-0.30024				
				<0.0001	0.0009			0.0001	0.0055				
73107985	73243368	Lclat1	lysocardiolipin acyltransferase 1			0.32324		-0.38733	-0.27215		0.27580	0.50208	0.40269
						0.0027		0.0003	0.0123		0.0111	<0.0001	0.0001
74338987	74391113	Spastin	spastin	0.34351	0.47480	0.23584							
				0.0014	<0.0001	0.0308							

* a (-) sign denotes a negative correlation between delta CT value and the trait, which indicates a positive association between mRNA expression and the trait. Blast. Denotes blastocyst. Of the 36 genes tested for correlations on the initial 6 BxD strains (Table S6), 26 were selected for analysis on all 28 BxD strains. Correlations were tested with and without parental strain data included. Data for significant correlations are shown. Map coordinates are from build 38.

Table S8. Significant pairwise correlations for selected genes in mRNA expression in MII stage oocytes using B6, D2, B6D2 F1 and BXD strains

Function	Chr	Gene	Digap1	Arhgap28	Mfsd9	Tmem182	Ndc80	Ypel5	Spast	Txnd9	Ccne2	Tbcl8	Pdcl3	Runx11	Chd7	Smchd1	Tgfr1	Esrp1	Phf3	Car8	Asph	Eif5b	Rab2a	Lclat1
		17 Epb4.113	0.0191	(<0.0001)	0.0012		(0.0165)	<0.0001	(0.0008)	(0.0002)				<0.0001	<0.0001	(0.0001)		<0.0001	(0.0005)			(0.0037)		
		17 Digap1		0.0013	0.0103	(<0.0001)	0.0055			(0.0009)	(0.0069)		(0.0021)		<0.0001		(0.0021)	0.0001		<0.0001		(<0.0001)	0.0301	
		17 Arhgap28					<0.0001	<0.0001	<0.0001		(0.0033)		(<0.0001)			<0.0001			0.0077	0.0002				(0.0029)
		1 Mfsd9				0.0037	0.0007			(0.0082)			0.0047				0.0047		(0.0002)					
		1 Tmem182					<0.0001									0.0034	0.0281							
		17 Ndc80						(<0.0001)	0.0004		(0.0157)	0.026				<0.0001				0.0261		0.0009		
		17 Ypel5												0.0344	0.0221	(<0.0001)	0.0091	<0.0001	(0.0012)	(0.0274)	0.0446	<0.0001		0.0017
		17 Spast							(<0.0001)		0.0059					0.0022	(0.0006)				0.0454	0.0111		
		1 Txnd9										0.006			(0.0073)	0.0037	0.0005	(<0.0001)				<0.0001		
		4 Ccne2															0.0188	0.0164	0.0009	(<0.0001)	0.0261		<0.0001	
		1 Tbcl8												0.0002				0.0186			<0.0001	0.0005		0.0152
		1 Pdcl3												0.001	(0.0114)	(0.0034)				(0.0203)		0.0442		
		4 Runx11													<0.0001	(0.0001)		0.005	(0.0004)		0.005	0.001		
		4 Chd7																	(0.0048)					
		17 Smchd1																		0.0015		0.0161		
		17 Tgfr1																			0.0005			0.0141
		4 Esrp1																						0.0024
		1 Phf3																			(<0.0001)			<0.0001
		4 Car8																						
		4 Asph																			(0.0007)			
		1 Eif5b																				0.0016		<0.0001
		4 Rab2a																						
		17 Lclat1																						

Values in () denote negative correlations; Bold font denotes genes in or near significance intervals. Bold font denotes the five strongest candidates for effects.

For the genes assayed by qRT-PCR for all 28 BXD strains and parental genotypes, values indicate significant correlations in oocyte mRNA expression amongst the different genotypes.

Table S9. Biofunction analysis of the 26 genes displaying significant associations between expression and developmental outcomes, and associations with biofunctions, two or more per category*

Category	Function	Function Annotation	p-value	Molecules	# Molecules
Cancer	infection	infection of cervical cancer cell lines	3.80E-03	DLGAP1, PHF3, RAB2A, SPAST	4
Reproductive System Disease	infection	infection of cervical cancer cell lines	3.80E-03	DLGAP1, PHF3, RAB2A, SPAST	4
Infectious Disease	infection	infection of cervical cancer cell lines	3.80E-03	DLGAP1, PHF3, RAB2A, SPAST	4
Infectious Disease	infection	infection by HIV-1	1.25E-02	DLGAP1, PHF3, RAB2A, SPAST	4
Embryonic Development	morphogenesis	morphogenesis of limb	3.74E-04	AFF3, ASPH, CHD7	3
Organismal Development	morphogenesis	morphogenesis of limb	3.74E-04	AFF3, ASPH, CHD7	3
Skeletal and Muscular System Development and Function	morphogenesis	morphogenesis of limb	3.74E-04	AFF3, ASPH, CHD7	3
Cancer	prostatic carcinoma	prostatic carcinoma	4.73E-03	ASPH, DLGAP1, EPB41L3	3
Reproductive System Disease	prostatic carcinoma	prostatic carcinoma	4.73E-03	ASPH, DLGAP1, EPB41L3	3
Embryonic Development	morphogenesis	morphogenesis of hindlimb	8.05E-04	AFF3, CHD7	2
Embryonic Development	development	development of face	1.57E-03	ASPH, CHD7	2
Organismal Development	morphogenesis	morphogenesis of hindlimb	8.05E-04	AFF3, CHD7	2
Organismal Development	development	development of face	1.57E-03	ASPH, CHD7	2
Organismal Development	morphology	morphology of face	1.45E-02	ASPH, TGIF1	2
Skeletal and Muscular System Development and Function	morphogenesis	morphogenesis of hindlimb	8.05E-04	AFF3, CHD7	2
Digestive System Development and Function	development	development of palate	3.37E-03	ASPH, CHD7	2
Nervous System Development and Function	abnormal morphology	abnormal morphology of axons	4.14E-03	EPB41L3, SPAST	2
Neurological Disease	gait disturbance	gait disturbance	9.53E-03	EPB41L3, SPAST	2
Neurological Disease	ataxia	ataxia	2.09E-02	CA8, EPB41L3	2
Tissue Morphology	abnormal morphology	abnormal morphology of axons	4.14E-03	EPB41L3, SPAST	2
Respiratory System Development and Function	abnormal morphology	abnormal morphology of snout	2.27E-03	ASPH, TGIF1	2
Cell Cycle	checkpoint control	checkpoint control	5.32E-03	CCNE2, NDC80	2
Hematological System Development and Function	circulation	circulation of blood	3.94E-03	CHD7, TBC1D8	2
DNA Replication, Recombination, and Repair	checkpoint control	checkpoint control	5.32E-03	CCNE2, NDC80	2
Cell Morphology	abnormal morphology	abnormal morphology of axons	4.14E-03	EPB41L3, SPAST	2
Gene Expression	repression	repression of RNA	2.35E-02	RUNX1T1, TGIF1	2

*Data were analyzed using the Ingenuity Pathway Analysis program.

Table S10. Gene polymorphisms affecting coding regions. The C57BL/6 and DBA/2 coding sequence data were compared for the 26 focus genes. Non-synonymous SNPs, insertions, or deletions were identified in the coding regions of the genes indicated.

Arhgap28	268970 Chr17	1
NM_172964.4 > NP_766552.3		
Non-syn. SNP at Chr17:68250679, AA #95 S -> A		
Indel in coding region at Chr17:68250659, [A,+GCAGCAGCC]:		
insertion of 9bp, inserts 3 AAs, replaces AA #101 "T"->"TAAA"		
B6	1 mevedsggvltayhsharsqpqgaeprcasrashplsrsksiprcrrinrmlsneslhpp	60
D2	1 mevedsggvltayhsharsqpqgaeprcasrashplsrsksiprcrrinrmlsneslhpp	60
B6	61 sfsrsnsqasvdssasmeefreiesikessvgaSqeppT---aaaaaevkpvdegel	117
D2	61 sfsrsnsqasvdssasmeefreiesikessvgaAqeppTAAaaaaaevkpvdegel	120
B6	118 eaewlqdvglstlisgneedgkallstlrrtqaaavkkryntyqtlrkknkqpvrdrv	177
D2	121 eaewlqdvglstlisgneedgkallstlrrtqaaavkkryntyqtlrkknkqpvrdrv	180
B6	178 difgvsespdscehatqldgtkeekdlpgvtktsrplpddaslstltsngaqdeegg	237
D2	181 difgvsespdscehatqldgtkeekdlpgvtktsrplpddaslstltsngaqdeegg	240
B6	238 fvalqsgsvsileaipdiavhtngsadaeqsvqstlsdddhygknvpaeaeelsfevsys	297
D2	241 fvalqsgsvsileaipdiavhtngsadaeqsvqstlsdddhygknvpaeaeelsfevsys	300
B6	298 emvtempdrnkwwksdikedylvtkfiqktrfgltetgdsvedmkkirhlsielta	357
D2	301 emvtempdrnkwwksdikedylvtkfiqktrfgltetgdsvedmkkirhlsielta	360
B6	358 ffdafgiqlkrnktervrgrdngifgvplvlldnrkkdpavkvpvlvqkffkveesg	417
D2	361 ffdafgiqlkrnktervrgrdngifgvplvlldnrkkdpavkvpvlvqkffkveesg	420
B6	418 lesegifrlsgctakvkqyreeldarfnadkfkwdkmchreaavmlkaffrelpstsifpv	477
D2	421 lesegifrlsgctakvkqyreeldarfnadkfkwdkmchreaavmlkaffrelpstsifpv	480
B6	478 eyipafismergpdikvqfqlhlmvmalpdanrdtaqalmaffnkvianesknrmnlw	537
D2	481 eyipafismergpdikvqfqlhlmvmalpdanrdtaqalmaffnkvianesknrmnlw	540
B6	538 nistvmapnlffsrskhsdceellantathiirmlkyqkilwkvpsflitqvrmmnea	597
D2	541 nistvmapnlffsrskhsdceellantathiirmlkyqkilwkvpsflitqvrmmnea	600
B6	598 tmlkkqlpsmkllrrktldrevsiltskvpqkpsrrmsdvppegvirvhapllskv	657
D2	601 tmlkkqlpsmkllrrktldrevsiltskvpqkpsrrmsdvppegvirvhapllskv	660
B6	658 smaiqlnsqtakdilakfyenshgsehikmqnrlyevggnigqhcldpdayildvy	717
D2	661 smaiqlnsqtakdilakfyenshgsehikmqnrlyevggnigqhcldpdayildvy	720
B6	718 hinphaewwikip	729
D2	721 hinphaewwikip	732

Phf3 213109 Chr1 1

NM_001081080.1 > NP_001074549.1

Non-syn. SNP at Chr1:30887618, AA #398 R -> Q

Non-syn. SNP at Chr1:30887279, AA #511 G -> D

Non-syn. SNP at Chr1:30878015, AA #860 T -> A

Indel in coding region at Chr1:30861870, [TGCCGCTCCCGCTCCC,-GCCGCTCCCGCTCCC]:
deletion of 15bp, removes 5 AAs (#1613-#1617, "GSGSG"->"")

B6 1 mdivdtfnhliptehlddalflgslenevcedfstsqnvledslknmlsddkdpmlgsas 60
D2 1 mdivdtfnhliptehlddalflgslenevcedfstsqnvledslknmlsddkdpmlgsas 60

B6 61 nqfclpvldsndpnfmpcstvvglldimdegvkesgndtideeelilpnrsldrved 120
D2 61 nqfclpvldsndpnfmpcstvvglldimdegvkesgndtideeelilpnrsldrved 120

B6 121 nsvrprksprlmaeqvrslrqstiaakrnaatlstkkpsgkltstskvgvkpaercqg 180
D2 121 nsvrprksprlmaeqvrslrqstiaakrnaatlstkkpsgkltstskvgvkpaercqg 180

B6 181 keevyaslkehpkerrsrghaeqmdvapevsassvssvscagmkeaeafdphacn 240
D2 181 keevyaslkehpkerrsrghaeqmdvapevsassvssvscagmkeaeafdphacn 240

B6 241 nqgevnvpseldcpllsetsasveekniealmeckaktntssplfkfpvredesqdlvsg 300
D2 241 nqgevnvpseldcpllsetsasveekniealmeckaktntssplfkfpvredesqdlvsg 300

B6 301 elndtiegdaggkpdqeseevkfpcgdqtaeepssdvssdsacanknaeknegaec 360
D2 301 elndtiegdaggkpdqeseevkfpcgdqtaeepssdvssdsacanknaeknegaec 360

B6 361 hlelknvdivdkpensqrneletlgygedtesndaRlqstefnksdleevdacafepe 420
D2 361 hlelknvdivdkpensqrneletlgygedtesndaRlqstefnksdleevdacafepe 420

B6 421 astlenticdvdqnsqlnitqsikmetanlqddrsglepknkpkhiksvthskqsm 480
D2 421 astlenticdvdqnsqlnitqsikmetanlqddrsglepknkpkhiksvthskqsm 480

B6 481 tetprktvaakhevghsktsknvavrnsGepeppdsqrpvkrkkqgdvkwksqscn 540
D2 481 tetprktvaakhevghsktsknvavrnsDepeppdsqrpvkrkkqgdvkwksqscn 540

B6 541 sgvksvksqahsvlkrmpdqntmqiskplthphsdklhghsgskepphvtghlvhs 600
D2 541 sgvksvksqahsvlkrmpdqntmqiskplthphsdklhghsgskepphvtghlvhs 600

B6 601 sqkqsqkppqqaavgksshvkdhdhpvsehkkeddklprkpdnrlqprrrsrfs 660
D2 601 sqkqsqkppqqaavgksshvkdhdhpvsehkkeddklprkpdnrlqprrrsrfs 660

B6 661 ldepplifpdniatvkkegsdqtsieskymwtpskqcgfckkphgnrfmvgrcddwf 720
D2 661 ldepplifpdniatvkkegsdqtsieskymwtpskqcgfckkphgnrfmvgrcddwf 720

B6 721 hgdvglslsqaqqmgeedkeyvcvccaedkktildteifeaqapieahsedkrmec 780
D2 721 hgdvglslsqaqqmgeedkeyvcvccaedkktildteifeaqapieahsedkrmec 780

B6 781 gkltsskhavtdkhrhsddpgkhkvilkresgegtssdsrdneikkwqlaplrlsq 840
D2 781 gkltsskhavtdkhrhsddpgkhkvilkresgegtssdsrdneikkwqlaplrlsq 840

B6 841 phlprsrseeksekiakesTalastgervarsgthekqetkkkkmekggpnvhppaatsk 900
D2 841 phlprsrseeksekiakesAalastgervarsgthekqetkkkkmekggpnvhppaatsk 900

B6 901 psadqirqsvrhlkdilmkrldtsnlkipeekaakvatkieelfsffrdtdakyknky 960
D2 901 psadqirqsvrhlkdilmkrldtsnlkipeekaakvatkieelfsffrdtdakyknky 960

B6 961 rslmfnlkdpknnilfkvlkgevtpdhlirmspeelaskelaawrrrenrhtiemieke 1020
D2 961 rslmfnlkdpknnilfkvlkgevtpdhlirmspeelaskelaawrrrenrhtiemieke 1020

B6 1021 qreverrppitkithkgeieiesdapmkeqeaaiieiqepsanksmekpdvsekqkeevdst 1080
D2 1021 qreverrppitkithkgeieiesdapmkeqeaaiieiqepsanksmekpdvsekqkeevdst 1080

B6 1081 skdttsqhrqhlfdlnckicigrmappiddlspktvkvvggarkhsdneasladaals 1140
D2 1081 skdttsqhrqhlfdlnckicigrmappiddlspktvkvvggarkhsdneasladaals 1140

B6 1141 ttniltsdlfeekqespkstfsptprmpgtvestflarlnfiwkgfinmpsvakf 1200
D2 1141 ttniltsdlfeekqespkstfsptprmpgtvestflarlnfiwkgfinmpsvakf 1200

B6 1201 vtkaypvsgspeyltedlpdsiqvgrispqtvwdyvekikasgtkeicvvrftpvteed 1260
D2 1201 vtkaypvsgspeyltedlpdsiqvgrispqtvwdyvekikasgtkeicvvrftpvteed 1260

B6 1261 qisytlfayfssrkrygvaanmkqvkdmlylipgaadkiphlplvpfdgpglelhrpnl 1320
D2 1261 qisytlfayfssrkrygvaanmkqvkdmlylipgaadkiphlplvpfdgpglelhrpnl 1320

B6 1321 llgliirqklkrphsasagpshtgetpesapivlppdkkgkmescteeaaeesdffnsf 1380
D2 1321 llgliirqklkrphsasagpshtgetpesapivlppdkkgkmescteeaaeesdffnsf 1380

B6 1381 ttvlhkqrnkpsqplqedlptaaplmevtkqepkplrflpgvligwdnqpstlelank 1440
D2 1381 ttvlhkqrnkpsqplqedlptaaplmevtkqepkplrflpgvligwdnqpstlelank 1440

B6 1441 plpvddilqslgttgqvyeqaaplveqstkeipfindqanpkvekikdkevtgedake 1500
D2 1441 plpvddilqslgttgqvyeqaaplveqstkeipfindqanpkvekikdkevtgedake 1500

B6 1501 ikvkaenisvstsknsgeetssvgssispgplaslrlgkppdvsteaftnlispskq 1560
D2 1501 ikvkaenisvstsknsgeetssvgssispgplaslrlgkppdvsteaftnlispskq 1560

B6 1561 eesvenkertlkrlllqdqenslqdnrtssdpcwpgtgkkgmdgdgsgsgsGSGSGseg 1620
D2 1561 eesvenkertlkrlllqdqenslqdnrtssdpcwpgtgkkgmdgdgsgsgs-----seg 1615

B6 1621 pvantrapqfinlkrdrprqaagrsqqtaseskdaescrngdkhaasapphnkeplaeavg 1680
D2 1616 pvantrapqfinlkrdrprqaagrsqqtaseskdaescrngdkhaasapphnkeplaeavg 1675

B6 1681 gegklpsqekssveqnddseaapnsssvvenlssqaeqanpsqedvltqnietvhpfr 1740
D2 1676 gegklpsqekssveqnddseaapnsssvvenlssqaeqanpsqedvltqnietvhpfr 1735

B6 1741 gsaptssrfeeggntcsefpsksvsftcrsssprastnfsmpmqpnlqhlkssppgfp 1800
D2 1736 gsaptssrfeeggntcsefpsksvsftcrsssprastnfsmpmqpnlqhlkssppgfp 1795

B6 1801 fpgpqnfppqnmfgfpphlsppllpppgfgfpqnpmpvppvhpvgppqrmmgplsqs 1860
D2 1796 fpgpqnfppqnmfgfpphlsppllpppgfgfpqnpmpvppvhpvgppqrmmgplsqs 1855

B6 1861 rymgpqnyfyqvkdirrperrhsdpwgrdqddrpfnrkgdrqrfysdshlkrerhd 1920
D2 1856 rymgpqnyfyqvkdirrperrhsdpwgrdqddrpfnrkgdrqrfysdshlkrerhd 1915

B6 1921 kdweqeserhrdrsqerdrdrkskeaaahkdkerprlshgdrapdgkasrdgksadk 1980
D2 1916 kdweqeserhrdrsqerdrdrkskeaaahkdkerprlshgdrapdgkasrdgksadk 1975

B6 1981 kpdprkgedhekekerdkskhkegedreryhkdrdhtdrvkskr 2025
D2 1976 kpdprkgedhekekerdkskhkegedreryhkdrdhtdrvkskr 2020

Pdcl3 68833 Chr1 1

NM_026850.4 > NP_081126.2
Non-syn. SNP at Chr1:39053052, AA #216 P -> L

B6 1 mqpndatwendiirrkkgilppkesleleeeaekeeqllqqsvvktvedmtleelen 60
D2 1 mqpndatwendiirrkkgilppkesleleeeaekeeqllqqsvvktvedmtleelen 60

B6 61 edefseederaiemyrqqlaewkatqlknkfgveisgkdyvqevtkageglwviihl 120
D2 61 edefseederaiemyrqqlaewkatqlknkfgveisgkdyvqevtkageglwviihl 120

B6 121 ykqgipclsinhhslgarkfpdvkikaisttcipnypdrnlptvfvyregdikaqfi 180
D2 121 ykqgipclsinhhslgarkfpdvkikaisttcipnypdrnlptvfvyregdikaqfi 180

B6 181 gplvfggmnlidewlksesgaiktaleenpkkPiqdllssvrgpvpmmrdsdsedd 240
D2 181 gplvfggmnlidewlksesgaiktaleenpkkLiqdllssvrgpvpmmrdsdsedd 240

Ndc80 67052 Chr17 1

NM_023294.2 > NP_075783.2
Non-syn. SNP at Chr17:71861782, AA #274 A -> E

B6 1 mkrsvstcgagrlsmqelrtldlnkpglytpqtkerstfgklsthkptserkvsifgkr 60
D2 1 mkrsvstcgagrlsmqelrtldlnkpglytpqtkerstfgklsthkptserkvsifgkr 60

B6 61 tsghsrnsqgifsseikidprplndkafiqqcirqlyeftengyvsvmskqlqap 120
D2 61 tsghsrnsqgifsseikidprplndkafiqqcirqlyeftengyvsvmskqlqap 120

B6 121 stkeflkifaflygflcpsyelpgtkceevprifkalgypftlskssmytvgaphtwph 180
D2 121 stkeflkifaflygflcpsyelpgtkceevprifkalgypftlskssmytvgaphtwph 180

B6 181 ivaalvwlidcikidtamkessplfdgqlwgeetedgikhnklfleytkkcyekfmtga 240
D2 181 ivaalvwlidcikidtamkessplfdgqlwgeetedgikhnklfleytkkcyekfmtga 240

B6 241 dsfeeedaelqakldlykvdasklesleankenAlneqiarleerereprnlmslkkk 300
D2 241 dsfeeedaelqakldlykvdasklesleankenElneqiarleerereprnlmslkkk 300

B6 301 aslqadvqnykaymsnleshavlqksnsdeeiqrveqecetvkqentrlqsvdnqk 360
D2 301 aslqadvqnykaymsnleshavlqksnsdeeiqrveqecetvkqentrlqsvdnqk 360

B6 361 ysvadierinheknelqqtinktkdleaeeqqmwneelkyargkeaeaqiaeyhklar 420
D2 361 ysvadierinheknelqqtinktkdleaeeqqmwneelkyargkeaeaqiaeyhklar 420

B6 421 kklipkgaenskydfeikfnpeaganclvkyrtqvyapkellnseeeinkalnkr 480
D2 421 kklipkgaenskydfeikfnpeaganclvkyrtqvyapkellnseeeinkalnkr 480

B6 481 hledtleqlntmkteskntvrmlkeeiqklddlhqqavkaeekdkksaseleslekhkh 540
D2 481 hledtleqlntmkteskntvrmlkeeiqklddlhqqavkaeekdkksaseleslekhkh 540

B6 541 llesgvndglseamdeldavqreyqltvkttteerrkvennlqrllmavthvgslekhl 600
D2 541 llesgvndglseamdeldavqreyqltvkttteerrkvennlqrllmavthvgslekhl 600

B6 601 eenakadreyeefmsedlleniremaekykrnaaqlkapdk 642
D2 601 eenakadreyeefmsedlleniremaekykrnaaqlkapdk 642

Spast 50850 Chr17 2

NM_001162870.1 > NP_001156342.1
Non-syn. SNP at Chr17:74738687, AA #104 E -> A

B6 1 msspagrrkkksggaspaparppppaavpapaagpapaagsppknpssfsplvgfa 60
D2 1 msspagrrkkksggaspaparppppaavpapaagpapaagsppknpssfsplvgfa 60

B6 61 llrlachlglfawlcqrfsralmaakrsgtapapaspppEpgpggeaesrvfhkq 120
D2 61 llrlachlglfawlcqrfsralmaakrsgtapapaspppApgpggeaesrvfhkq 120

B6 121 afeyisialrideeekagqkeqavewykgieelekgiavivtgqgeqyerarrlqakmm 180
D2 121 afeyisialrideeekagqkeqavewykgieelekgiavivtgqgeqyerarrlqakmm 180

B6 181 tnlvmakdrllqleklqplvlfqsksqtdvynestnltrcnhlqsesgavprkrkdpltha 240
D2 181 tnlvmakdrllqleklqplvlfqsksqtdvynestnltrcnhlqsesgavprkrkdpltha 240

B6 241 snslprsktvksgsaglsghhrapscsglsmvsgarppgpaatthkgtkpnrtnkps 300
D2 241 snslprsktvksgsaglsghhrapscsglsmvsgarppgpaatthkgtkpnrtnkps 300

B6 301 tpttavrrkkdknfrnvdnsnlanlimneivdngtavkfdiagqelakqalqeilps 360
D2 301 tpttavrrkkdknfrnvdnsnlanlimneivdngtavkfdiagqelakqalqeilps 360

B6 361 lrpelftglrapargllfpgpngktmlakavaaesnatffnisaasitskyvgegekl 420
D2 361 lrpelftglrapargllfpgpngktmlakavaaesnatffnisaasitskyvgegekl 420

B6 421 vralfavarelqpsiiifidevdsllcerregehdasrrlktefliefdgvqsagddrvlv 480
D2 421 vralfavarelqpsiiifidevdsllcerregehdasrrlktefliefdgvqsagddrvlv 480

B6 481 mgatnrpqeldeavrrfikrvyvspneetrllllknllckqgspltqkelaqlarmtd 540
D2 481 mgatnrpqeldeavrrfikrvyvspneetrllllknllckqgspltqkelaqlarmtd 540

B6 541 gysgsdltalakdaalgpirelkeqvknsasemnrnlsdfteslkkikrsvspqtle 600
D2 541 gysgsdltalakdaalgpirelkeqvknsasemnrnlsdfteslkkikrsvspqtle 600

B6 601 ayirwnkdfgdttv 614
D2 601 ayirwnkdfgdttv 614

NM_016962.2 > NP_058658.2
Non-syn. SNP at Chr17:74738687, AA #104 E -> A

B6 1 msspagrrkkksggaspaparppppaavpapaagpapaagsppknpssfsplvgfa 60
D2 1 msspagrrkkksggaspaparppppaavpapaagpapaagsppknpssfsplvgfa 60

B6 61 llrllachlgllfawlcqrfsrmaakrsgstapapaspsppEpppggeaesvrvfhkq 120
D2 61 llrllachlgllfawlcqrfsrmaakrsgstapapaspsppApppggeaesvrvfhkq 120

B6 121 afeyisialrideeekgqkeqavevykkgieelekgiavivtgqgeqyerarrlqakmmt 180
D2 121 afeyisialrideeekgqkeqavevykkgieelekgiavivtgqgeqyerarrlqakmmt 180

B6 181 nlvmakdrllqleklqpvlfqfsksqtdvynestnltrnglqssegavpkrkdpthas 240
D2 181 nlvmakdrllqleklqpvlfqfsksqtdvynestnltrnglqssegavpkrkdpthas 240

B6 241 nslprsktvksgsaglsghhrapsccsglsmvsgarpggpaatthkgtkpnrtkpkst 300
D2 241 nslprsktvksgsaglsghhrapsccsglsmvsgarpggpaatthkgtkpnrtkpkst 300

B6 301 pttavrkkkdlknfrnvdsnlanlimneivdngtavkfddiagqelakqalqeivilpsi 360
D2 301 pttavrkkkdlknfrnvdsnlanlimneivdngtavkfddiagqelakqalqeivilpsi 360

B6 361 rpelftgraparglllfgppgngktmlakavaaesnatffnisaaslskyvgegeklv 420
D2 361 rpelftgraparglllfgppgngktmlakavaaesnatffnisaaslskyvgegeklv 420

B6 421 ralfavarelqpsiifidevdsllcerregehdasrrktefliefdgvqsagddrvlvm 480
D2 421 ralfavarelqpsiifidevdsllcerregehdasrrktefliefdgvqsagddrvlvm 480

B6 481 gatnrrpqeldeavlrrikrvyvslnpneetrllllknllckqgspltqkelaqlarntdg 540
D2 481 gatnrrpqeldeavlrrikrvyvslnpneetrllllknllckqgspltqkelaqlarntdg 540

B6 541 ysgsdltalakdaalgpirelkepvknmsasemnrilsdfteslkkikrsvspqtlea 600
D2 541 ysgsdltalakdaalgpirelkepvknmsasemnrilsdfteslkkikrsvspqtlea 600

B6 601 yirwnkdfgdttv 613
D2 601 yirwnkdfgdttv 613
